

Thin-bed Resolution from Cepstrum Analysis

by

Robert A. Bryan

Thesis submitted to the Faculty of the  
Virginia Polytechnic Institute and State University  
in partial fulfillment of the requirements for the degree of  
Master of Science  
in  
Department of Geological Sciences

APPROVED:

\_\_\_\_\_  
J. K. Costain, Chairman

\_\_\_\_\_  
C. Cøruh

\_\_\_\_\_  
E. S. Robinson

\_\_\_\_\_  
J. A. Snøke

August 7, 1985  
Blacksburg, Virginia

## Thin-bed Resolution from Cepstrum Analysis

by

Robert A. Bryan

J. K. Costain, Chairman

Department of Geological Sciences

(ABSTRACT)

A method of cepstrum analysis is developed for the purpose of resolving thin-beds. The method relies on the detection of periodic pulses of the cepstra of reflectivity functions, which are isolated by computing a sub-cepstrum and a sum-cepstrum, and highlighted with a discriminator, where the sub-cepstrum of the functions  $f_1(t)$  and  $f_2(t)$  is the difference between the cepstra of the two functions, the sum-cepstrum of  $f_1(t)$  is the sum of the sub-cepstra of  $f_1(t)$  and  $f_k(t)$ ,  $k=2,3,4,\dots$ , and the discriminator is the product of the sum-cepstrum and the autocovariance of the sum-cepstrum. The technique requires at least two reflected wavelets generated by the same source.

The method was applied to synthetic thin lens models. The method is shown to be sensitive to the ratio of the reflection coefficients at the top and bottom of the thin-bed. Specifically, the resolution depends on the ratio of the reflection coefficients. Optimum resolution is achieved when the reflection coefficients at the top and bottom of the thin-bed are equal in absolute magnitude. In addition, in

the noise-free case, the absolute magnitude of the cepstral pulses can be used to determine the absolute magnitude of the ratio of the reflection coefficients. The technique is also sensitive to the sample interval used. The finest sample interval provides the best resolution because it produces the sharpest cepstral pulses and resolves the thinnest beds. The resolution of the method is drastically reduced by random noise, although thin-bed thicknesses are still detectable when the S/N of the synthetic seismic section is 15/1 and the upper frequency of the bandwidth of the noise is 1.1 octaves above the upper frequency of the bandwidth of the source wavelet.

## ACKNOWLEDGEMENTS

The patience and enthusiasm of Dr. J. K. Costain and Dr. C. Coruh are deeply appreciated and admired. Their suggestions and criticism have been essential to this work. I would like to thank Dr. E. S. Robinson and Dr. J. A. Snoke for their critique of the text.

I am thankful to \_\_\_\_\_ and \_\_\_\_\_ for their assistance with the VAX 11/780, and their encouragement.

I am grateful to the graduate students for their help during trying times. Thank-you \_\_\_\_\_ and \_\_\_\_\_ for your willingness to share knowledge.

I am grateful to Conoco Inc. for financial assistance provided during my enrollment at Virginia Polytechnic Institute and State University.

I would like to thank the Thin-bed Consortium, comprised of the following members; Champlin Petroleum Co., Chevron USA, Inc., Conoco Inc., Getty Oil Co., Phillips Petroleum Co. and Sohio Petroleum Co., for helping to fund this study.

To my family,  
whose love has been my wings.

# TABLE OF CONTENTS

INTRODUCTION . . . . .	1
THEORY . . . . .	3
The Cepstrum . . . . .	3
The Cepstrum of a Wavelet . . . . .	4
The Cepstra of a Dipole and Doublet . . . . .	6
The Spectrum of the Cepstrum . . . . .	9
Cepstrum Analysis of a Dipole and Doublet . . . . .	10
Reflection from a Thin Layer . . . . .	10
The Sub-cepstrum and Sum-cepstrum . . . . .	14
Periodicity Discriminator . . . . .	16
APPLICATION TO SYNTHETIC GEOLOGIC MODELS . . . . .	18
Synthetic Models: Thin Lens . . . . .	18
Resolution in the Quefreny Domain . . . . .	20
SUMMARY AND CONCLUSION . . . . .	70
PROPOSAL FOR FUTURE STUDIES . . . . .	72
REFERENCES . . . . .	74
Vita . . . . .	76

## LIST OF ILLUSTRATIONS

Figure 1. Spectra and cepstrum of doublet . . . . .	11
Figure 2. Spectra and cepstrum of dipole . . . . .	12
Figure 3. Depth section of synthetic model . . . . .	19
Figure 4. Lens Model 1 . . . . .	22
Figure 5. $ R_1/R_0 =1$ . . . . .	23
Figure 6. Lens Model 2 . . . . .	25
Figure 7. $ R_1/R_0 =3/4$ . . . . .	26
Figure 8. Lens Model 3 . . . . .	27
Figure 9. $ R_1/R_0 =1/2$ . . . . .	28
Figure 10. Lens Model 4 . . . . .	29
Figure 11. $ R_1/R_0 =1/4$ . . . . .	30
Figure 12. Lens Model 5 . . . . .	32
Figure 13. Reflectivity function of model 5 . . . . .	33
Figure 14. Source wavelet . . . . .	34
Figure 15. Lens Model 6 . . . . .	36
Figure 16. Reflections at CDP's 60 and 77 . . . . .	37
Figure 17. Analytic functions of reflections . . . . .	38
Figure 18. Reflectivity functions at CDP's 60 and 77 . . . . .	39
Figure 19. Sub-cepstrum of reflectivity functions . . . . .	40
Figure 20. Reflection at CDP 55 of Model 6 . . . . .	43
Figure 21. Reflection at CDP 55 (dt=1 ms) . . . . .	44
Figure 22. Reflection at CDP 55 (dt=2 ms) . . . . .	45
Figure 23. Reflection at CDP 77 of model 6 . . . . .	47
Figure 24. Reflection at CDP 77 (dt=1 ms) . . . . .	48
Figure 25. Reflection at CDP 77 (dt=2 ms) . . . . .	49

Figure 26. Synthetic noise . . . . .	51
Figure 27. Synthetic section with S/N of 15/1 . . . . .	53
Figure 28. Reflection without noise; CDP 55 . . . . .	55
Figure 29. Reflection without noise; CDP 57 . . . . .	56
Figure 30. Reflection without noise; CDP 70 . . . . .	57
Figure 31. Reflection without noise; CDP 71 . . . . .	58
Figure 32. Reflection without noise; CDP 76 . . . . .	59
Figure 33. Reflection without noise; CDP 77 . . . . .	60
Figure 34. Reflection with added noise; CDP 55 . . . . .	62
Figure 35. Reflection with added noise; CDP 57 . . . . .	63
Figure 36. Reflection with added noise; CDP 70 . . . . .	64
Figure 37. Reflection with added noise; CDP 71 . . . . .	65
Figure 38. Reflection with added noise; CDP 76 . . . . .	66
Figure 39. Reflection with added noise; CDP 77 . . . . .	67

## INTRODUCTION

One of the challenging problems of geophysics is the detection of thin-beds. Thin-beds such as coals seams and hydrocarbon bearing sand stringers are common thin-bed targets because of their economic value. Widess (1973) defines a thin-bed as a layer with a two-way traveltime less than one fourth the period,  $T$ , of the source wavelet in the bed. He showed that if the two-way traveltime in the bed decreased from  $T/4$  to 0 sec, the shape of the reflection would be virtually unchanged. Therefore resolving the thickness of a thin-bed by a traditional method of wave shape analysis is a formidable task.

An application of homomorphic analysis is developed herein for the purpose of resolving thin layers. The method is a form of cepstrum analysis, which relies on the detection of periodic pulses of the cepstrum of reflectivity functions. The method is advantageous because, as with homomorphic deconvolution (Ulyrch, 1971, Oppenheim and Schafer, 1975), it makes no assumptions about the source wavelet. However, unlike homomorphic deconvolution, the method discussed within avoids the problem of unwrapping the phase of the complex cepstrum (Jin and Eisner, 1984, Childer et al., 1977) by using only the cepstrum. The technique requires at least two reflected wavelets generated by the same source.

The method was tested on synthetic models of a thin lens. The results indicate that where numerous reflections from a thin-bed are available the method of cepstrum analysis can be effective. It is also shown that the resolution of the method is reduced by random noise when the bandwidth of the noise exceeds the bandwidth of the reflection.

## THEORY

### The Cepstrum

Let  $f(t)$  be a real time function with Fourier transform

$$F(\omega) = \int_{-\infty}^{\infty} f(t)\exp(-i\omega t)dt. \quad (1)$$

The complex cepstrum (Oppenheim and Schaffer, 1975) of  $f(t)$  is

$$\begin{aligned} x(t) &= (1/2\pi) \int_{-\infty}^{\infty} \ln[|F(\omega)|\exp(i\phi(\omega))]\exp(i\omega t)d\omega \quad (2) \\ &= (1/2\pi) \int_{-\infty}^{\infty} [\ln|F(\omega)| + i\phi(\omega)]\exp(i\omega t)d\omega \\ &= c(t) + i(1/2\pi) \int_{-\infty}^{\infty} \phi(\omega)\exp(i\omega t)d\omega \end{aligned}$$

where  $\phi(\omega)$  is the phase of  $F(\omega)$  and  $c(t)$  is the cepstrum (Bogert, Healy, and Tukey, 1963) of  $f(t)$ , and

$$\begin{aligned} c(t) &= (1/2\pi) \int_{-\infty}^{\infty} [\ln|F(\omega)|]\exp(i\omega t)d\omega \quad (3) \\ &= (x(t) + x(-t))/2. \end{aligned}$$

Whereas  $f(t)$  is in the time domain, the cepstrum and complex cepstrum are in the quefrequency domain.

### The Cepstrum of a Wavelet

If  $f(t)$  is a source wavelet its  $z$ -transform is (Oppenheim and Schafer, 1975, p 501)

$$F(z) = \frac{Az^r \prod_{k=1}^m (1 - a_k/z) \prod_{k=1}^{\mu} (1 - b_k z)}{\prod_{k=1}^p (1 - c_k/z) \prod_{k=1}^p (1 - d_k z)} \quad (4)$$

where  $|a_k|$ ,  $|b_k|$ ,  $|c_k|$ , and  $|d_k|$  are less than unity. If  $z$  is  $\exp(-i\omega)$ , then  $z=a_k$  and  $z=1/b_k$  are zeros outside and inside the unit circle, respectively, and  $z=c_k$  and  $z=1/d_k$  are poles outside and inside the unit circle.  $A$  is some real constant and  $z^r$  represents a time lag of  $r$  time units. If the wavelet has not been time shifted, as will be assumed,  $r$  is equal to 0. The logarithm of  $F(z)$  yields,

$$\begin{aligned}
\ln[F(z)] = \ln|A| & - \sum_{k=1}^m \sum_{n=1}^{\infty} a_k^n z^{-n}/n + \sum_{k=1}^p \sum_{n=1}^{\infty} c_k^n z^{-n}/n \\
& + \sum_{k=1}^{\mu} \sum_{n=1}^{\infty} b_k^n z^n/n - \sum_{k=1}^{\rho} \sum_{n=1}^{\infty} d_k^n z^n/n. \quad (5)
\end{aligned}$$

The absolute value of A is used in the logarithmic expression to insure that the operation is analytical. In arriving at the expression for  $\ln[F(z)]$  the following power series expansion was used;

$$\ln(a + by) = \sum_{m=0}^{\infty} (-1)^m (by)^{m+1} / (m+1) a^{m+1}; \quad |b| < |a|. \quad (6)$$

$\ln[F(z)]$  is the z-transform of the complex cepstrum,  $x(n)$ ; therefore,

$$x(0) = \ln|A| \quad (7a)$$

$$x(n) = -1/n \sum_{k=1}^m a_k^n + 1/n \sum_{k=1}^p c_k^n; \quad n > 0 \quad (7b)$$

$$x(n) = \frac{1}{n} \sum_{k=1}^{\mu} b_k^{-n} - \frac{1}{n} \sum_{k=1}^{\rho} d_k^{-n}; \quad n < 0. \quad (7c)$$

Then the cepstrum is

$$c(0) = \ln|A| \quad (8a)$$

$$c(n) = (1/2) \left[ -\frac{1}{n} \left( \sum_{k=1}^m a_k^n - \sum_{k=1}^p c_k^n \right) + \frac{1}{n} \left( \sum_{k=1}^{\mu} b_k^{-n} - \sum_{k=1}^{\rho} d_k^{-n} \right) \right]. \quad (8b)$$

The cepstrum,  $c(n)$ , and complex cepstrum,  $x(n)$ , of the wavelet decay at a rate that is proportional to  $1/n$ .

#### The Cepstra of a Dipole and Doublet

Now consider the reflectivity function,  $r(t)$ , where

$$r(t) = R_0 + R_1 \delta(t - \tau). \quad (9)$$

$R_0$  and  $R_1$  are the reflection coefficients at the top and bottom of a layer; respectively,  $\delta(t)$  is the kronecker delta

function, and  $\tau$  is the two-way traveltime through the layer.

The z-transform of  $r(t)$  is

$$R(z) = R_0 + R_1 z^\tau \quad (10)$$

The logarithm of  $R(z)$  is

$$\ln(R(z)) = \ln|R_0| + \sum_{n=1}^{\infty} (-1)^{n-1} (R_1/R_0)^n (z^{n\tau}/n);$$

$$|R_0| \geq |R_1| \quad (11)$$

or

$$\ln(R(z)) = \ln|R_1| + \sum_{n=1}^{\infty} (-1)^{n-1} (R_0/R_1)^n (z^{n\tau}/n);$$

$$|R_1| \geq |R_0|. \quad (12)$$

Then the complex cepstrum of  $r(t)$  is given by;

$$x(0) = \ln|R_0| \quad (13a)$$

$$x(t) = (-1)^{n-1}/n (R_1/R_0)^n \delta(t - n\tau);$$

$$|R_0| \geq |R_1|, n = \pm 1, 2, 3 \dots \quad (13b)$$

or

$$x(0) = \ln|R_1| \quad (14a)$$

$$x(t) = (-1)^{n-1}/n (R_0/R_1)^n \delta(t - n\tau);$$
$$|R_1| \geq |R_0|, n = \pm 1, 2, 3 \dots \quad (14b)$$

and the cepstrum is

$$c(0) = \ln|R_0| \quad (15a)$$

$$c(t) = ((-1)^{n-1}/2n) (R_1/R_0)^n \delta(t - n\tau);$$
$$|R_0| \geq |R_1|, n = \pm 1, 2, 3 \dots \quad (15b)$$

or

$$c(0) = \ln|R_1| \quad (16a)$$

$$c(t) = ((-1)^{n-1}/2n) (R_0/R_1)^n \delta(t - n\tau);$$
$$|R_1| \geq |R_0|, n = \pm 1, 2, 3 \dots \quad (16b)$$

The cepstrum has pulses at  $t=0$  and  $t=n\tau$ . In addition, the amplitudes of the pulses decay at a rate that is proportional to  $1/n$ ; therefore, the thickness of the layer can be determined from the time between decaying pulses of the cepstrum

of  $r(t)$  and the ratio  $R_0/R_1$  can be determined from equation (16b) in the noise-free case.

The cepstrum of  $r(t)$  will give the two-way travel time through a layer with a reflectivity function modeled by a dipole or a doublet. As used here, a dipole is a pair of reflection coefficients, not necessarily equal, of opposite polarity; a doublet is a pair of reflection coefficients of the same polarity. The formula for the cepstrum of the reflectivity function of a layer indicates that the evenly spaced pulses of the cepstrum of a dipole are negative, whereas, the adjacent, evenly spaced pulses of the cepstrum of a doublet are alternating positive and negative.

### The Spectrum of the Cepstrum

The first and second derivatives of  $\ln[R(z)]$  show that the amplitude spectrum of the cepstrum of a dipole or doublet has a fundamental period of  $1/\tau$ . In particular, the amplitude spectrum of the cepstrum of a dipole peaks at the following harmonic frequencies;

$$f_n = n/\tau \tag{17}$$

and the amplitude spectrum of the cepstrum of a doublet peaks at the following harmonic frequencies;

$$f_n = (2n + 1)/2\tau \quad (18)$$

Once recognized, the fundamental period of  $1/\tau$  can be used to compute the thickness of the layer.

### Cepstrum Analysis of a Dipole and Doublet

To illustrate the theoretical results, the cepstrum and spectra of a doublet and dipole with two-way traveltimes of 23.4 ms were computed and illustrated in Figure 1 and Figure 2. The frequency spectrum of each cepstrum has a fundamental period of approximately 42.7 Hz or  $1/23.4$  ms; for instance, the adjacent pulses of each cepstrum occur at an interval of 23.4 ms. Therefore, the layer thickness can be easily determined from analyses of the frequency spectrum and the cepstrum.

### Reflection from a Thin Layer

If  $s(t)$  is a reflection from a layer, then

$$s(t) = r(t)*f(t). \quad (19)$$

The z-transform of  $s(t)$  is

$$S(z) = F(z)R(z). \quad (20)$$

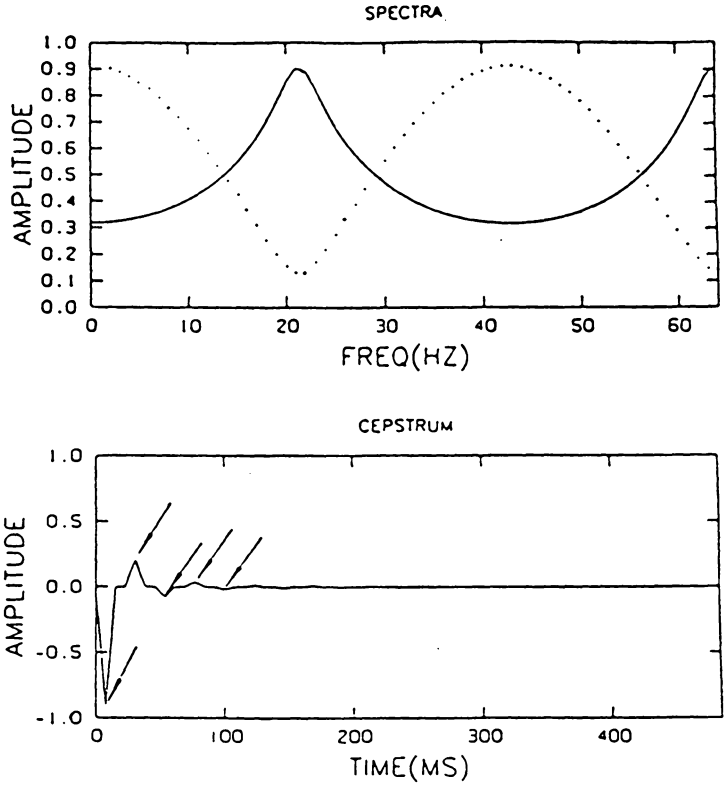
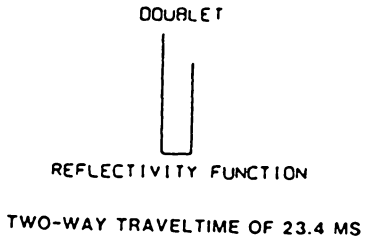


Figure 1. Spectra and cepstrum of doublet: Amplitude spectrum (solid line) of the cepstrum peaks at 21.3 HZ and 64.0 Hz. The amplitude spectrum of the doublet (dotted) has minima at 21.3 HZ and 64.0 Hz. The period of each spectrum, 42.7 HZ is equal to the reciprocal of the two-way traveltime, 23.4 ms. In addition, cepstral pulses (see arrows) occur ever Note that the vertical axes have been normalized such that the largest amplitude is 1.

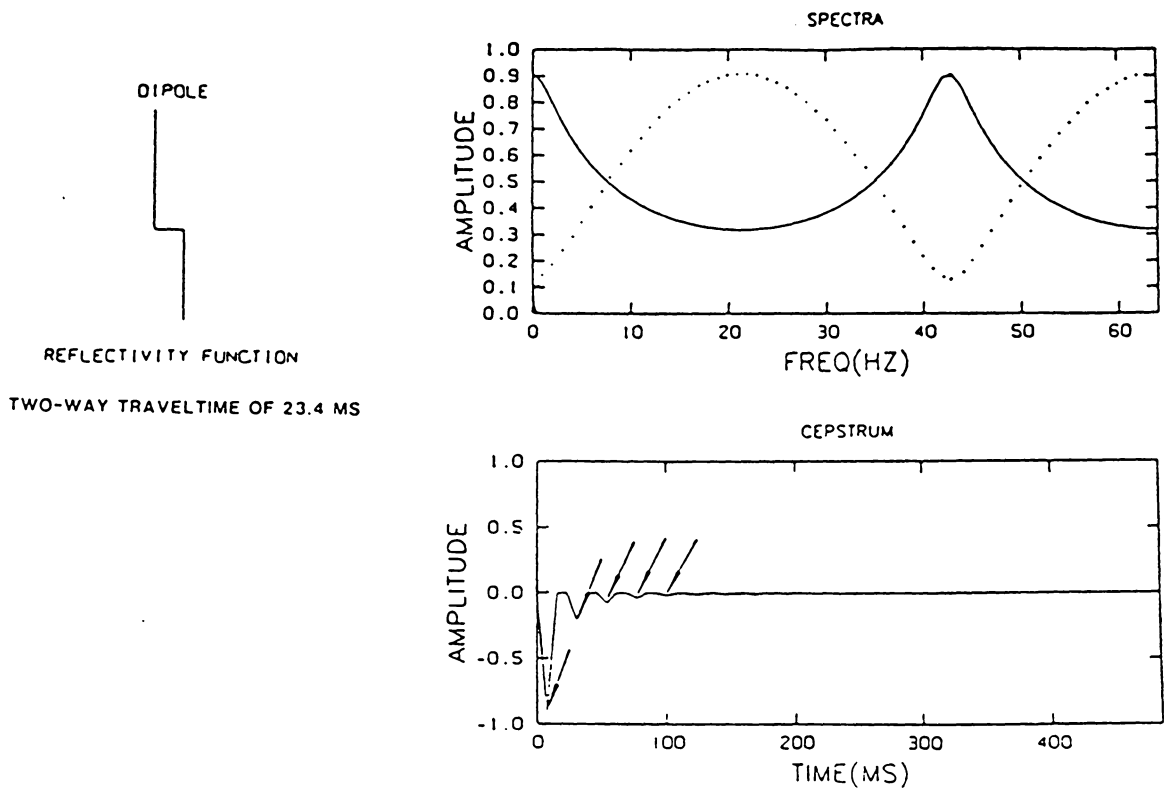


Figure 2. Spectra and cepstrum of dipole: Amplitude spectrum of the cepstrum peak at about 42.7 Hz. The amplitude spectrum (dotted) of the dipole has a minimum at 42.7 Hz. 42.7 Hz is equal to the reciprocal of the two-way traveltime, 23.4 ms. In addition, the cepstral pulses (see arrows) occur every 23.4 ms. Note that the vertical axes have been normalized such that the largest amplitude is 1.

Furthermore,

$$\ln[S(z)] = \ln[F(z)] + \ln[R(z)] \quad (21)$$

so that the cepstrum of the reflection is the sum of the cepstrum of the source wavelet and the cepstrum of the reflectivity function.

The cepstrum of the reflectivity function peaks periodically. Therefore, if the cepstrum of the source wavelet is smooth and flat in comparison to the cepstrum of the reflectivity function, the two-way traveltime can be determined from the periodic pulses of the cepstrum of the reflectivity function. However, if the cepstrum of the source wavelet is neither smooth nor flat, it will distort or completely obscure the periodic pulses of the cepstrum of the reflectivity function; thus limiting resolution in the quefreny domain. Resolution in the quefreny domain is dependent on the ease with which periodic cepstral pulses can be identified.

The resolution provided by the cepstrum of the reflectivity function also depends on the ratio of the magnitudes of the reflection coefficients. Specifically, the amplitudes of the cepstral pulses increases as  $|R_1/R_0|$  increases when  $|R_1| \leq |R_0|$  and as  $|R_0/R_1|$  increases when  $|R_0| \leq |R_1|$ .

## The Sub-cepstrum and Sum-cepstrum

Identifying the periodic pulses of the cepstrum can be facilitated by subtracting the cepstrum of the source wavelet from the cepstrum of the reflectivity function. If the source wavelet is known, then the cepstrum of the source wavelet can be computed and then subtracted from the cepstrum of the reflection; hence only the cepstrum of the reflectivity function will remain. However, if the source wavelet is unknown, the cepstrum of the source wavelet can be eliminated by subtracting the cepstra of two reflections each of which contains the same source wavelet. This is possible because convolution in the time domain is equivalent to addition in the quefreny domain. For example; let  $s_i(t)$  and  $s_j(t)$  be reflections generated by the source wavelet  $f(t)$ . The cepstrum of  $s_i(t)$  is

$$c_i(t) = c_{ri}(t) + c_f(t) \quad (22)$$

where  $c_{ri}(t)$  is the cepstrum of the reflectivity function,  $r_i(t)$ , and  $c_f(t)$  is the cepstrum of  $f(t)$ . Similarly, the cepstrum of  $s_j(t)$  is

$$c_j(t) = c_{rj}(t) + c_f(t) \quad (23)$$

where  $c_{rj}(t)$  is the cepstrum of the reflectivity function  $r_j(t)$ . Subtracting  $c_j(t)$  from  $c_i(t)$  gives;

$$B_{ij}(t) = c_{ri}(t) - c_{rj}(t) \quad (24)$$

For convenience,  $B_{ij}(t)$  will be referred to as a sub-cepstrum of  $s_i(t)$  and  $s_j(t)$ . As will be seen, there can be an infinite number of sub-cepstra of  $s_i(t)$ . If  $r_i(t)$  and  $r_j(t)$  are equal, then  $B_{ij}(t)$  is zero at all times,  $t$ . But assuming that  $r_i(t)$  and  $r_j(t)$  are any unequal combination of a dipole and doublet, then  $B_{ij}(t)$  contains the periodic pulses of the cepstrum of each reflectivity function.

The cepstral pulses of  $s_i(t)$  can be isolated by computing several sub-cepstra of  $s_i(t)$ . Each sub-cepstrum of  $s_i(t)$  will contain the periodic pulses of  $c_i(t)$ . If each of the sub-cepstrum is computed with a unique second reflection,  $s_k(t)$ ,  $k = 1, 2, 3, \dots$ , then the occurrence of the pulses of  $c_{ri}(t)$  in each sub-cepstrum confirms the reliability of these pulses as good indicators of the correct two-way traveltime corresponding to  $r_i(t)$ .

If the sub-cepstra are summed the amplitudes of the pulses of the  $c_{ri}(t)$ 's will increase relative to the amplitudes of the pulses of the  $c_{rk}(t)$ 's, as long as the pulses of the  $c_{rk}(t)$ 's do not always interfere constructively. The summation of the sub-cepstra can be expressed as;

$$\begin{aligned}
M_i^k(t) &= B_{i1}(t) + B_{i2}(t) + \dots + B_{ik}(t) \\
&= \sum_{j=1}^k B_{ij}(t) \\
&= kc_{ri}(t) - (c_{r1}(t) + c_{r2}(t) + \dots + c_{rk}(t)). \quad (25)
\end{aligned}$$

Hereafter the summation of the sub-cepstra of  $s_i(t)$  and  $s_k(t)$  function will be called the sum-cepstrum and  $s_i(t)$  will be called the reference trace.

### Periodicity Discriminator

A function has been defined to discriminate between the periodic and aperiodic amplitudes of the sum-cepstrum. The discriminating function is called the discriminator,  $D(t)$ . It is the product of the sum-cepstrum and the autocovariance of the sum-cepstrum. Therefore;

$$D(t) = M_i^k(t) \int_{-\infty}^{\infty} M_i^k(\tau) M_i^k(\tau-t) d\tau \quad (26)$$

The autocovariance of  $M_i^k(t)$  peaks at intervals of the dominant period of  $M_i^k(t)$ , so that the product of the two functions enhances the periodic pulses of the sum-cepstrum while smoothing the random intermediate amplitudes. Consequently

any periodicity of the sum-cepstrum also occurs in the discriminator.

## APPLICATION TO SYNTHETIC GEOLOGIC MODELS

### Synthetic Models: Thin Lens

The method of cepstrum analysis discussed was applied to synthetic geologic models; four of which contain a thin high speed lens and one which contains a thin low speed lens. Each lens has an horizontal extent of 2000 m and a maximum thickness of 25 m. The depth section (Figure 3) corresponding to the lens models was created by AIMS® (Advance Interpretative Modeling System) version 3.0.

Reflection coefficients of the model were computed by using AIMS®. The reflection coefficients were generated while assuming a velocity of 4000 m/s within the lens, a velocity of 3000 m/s above and beneath the lens, and normal incidence raypaths from each interface of the lens.

Final two-way traveltimes sections were created by the modifying the reflection coefficients produced by AIMS®. It was necessary to change the AIMS® model because a reflection coefficient created by AIMS® is not a simple pole. A reflection coefficient generated by AIMS® is filtered such that in the amplitude spectrum of the reflection coefficient amplitudes at frequencies between 0 HZ and 4 HZ increase line-

---

®Registered trademark of GeoQuest International, Inc.

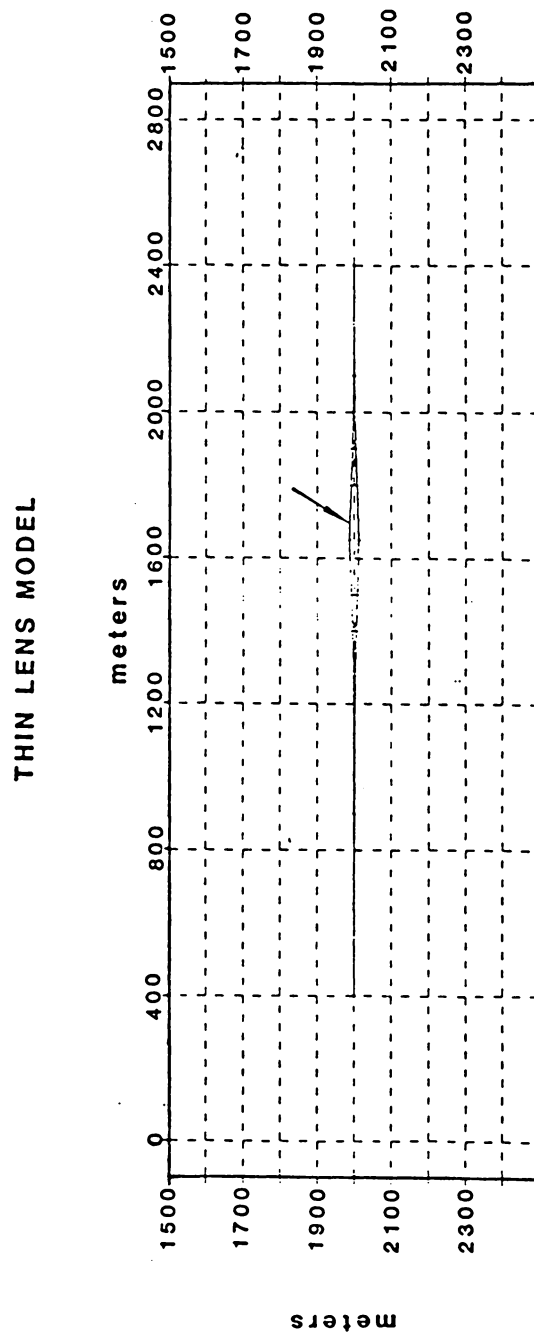


Figure 3. Depth section of synthetic model: Thin lens model created by AIMS®.

arly from 0 to 1 and amplitudes at frequencies between  $7/8$  the folding frequency and the folding frequency decrease linearly from 1 to 0; at all other frequencies the amplitude is 1. Consequently, the AIMS® reflection coefficient is a broad pulse containing at least two poles of same polarity. Accordingly, a layer modeled with AIMS® consists of at least four reflection coefficients, two at the upper interface and two at the lower interface. In contrast, conventionally a layer is modeled by two reflection coefficients, one at the top interface and one at the bottom interface, for instance by a dipole or doublet. Therefore, final two-way traveltime sections were created by changing the reflectivity functions produced by AIMS® to dipoles.

### Resolution in the Quefreny Domain

#### The effect of the ratio of the reflection coefficients

Given the cepstra of two reflectivity functions, each from a thin layer, the difference between the two cepstra is proportional to the difference between the ratios ( $R_1/R_0$  if  $|R_0| \leq |R_1|$ , or  $R_1/R_0$  if  $|R_1| \leq |R_0|$ ) of the respective coefficients. The difference between the two cepstra is

$$\begin{aligned}
 \Delta(t) &= ((-1)^{n/2n})(\alpha^n - \beta^n)\delta(t - n\tau) & (27) \\
 &= ((-1)^{n/2n})(\alpha^{n-1} + \alpha^{n-2}\beta + \alpha^{n-3}\beta^2 + \dots \\
 &\quad + \alpha\beta^{n-1} + \beta^{n-1})\delta(t - n\tau)(\alpha - \beta)
 \end{aligned}$$

where there are  $n$  terms in the expression.  $\alpha$  is the ratio of the reflection coefficients of one reflectivity function and  $\beta$  is the ratio of the reflection coefficients of the other reflectivity function. Because  $|\alpha| \leq 1$  and  $|\beta| \leq 1$ , as the difference between  $\alpha$  and  $\beta$  increases,  $\Delta(t)$  also increases at all times  $n\tau$ .

Using CDP 77 of models 1 through 4 as reference signals, it is shown that resolution in the quefreny domain is proportional to the ratio of the reflection coefficients. A sample interval of 1/2 ms was used to generate models 1 to 4.

#### Model 1

In model 1 ( Figure 4) the reflection coefficients of the lens are  $R_0=1$  and  $R_1=-1$ . Therefore at CDP 77  $|R_1/R_0|=1$  (Figure 5). The two-way travelttime at CDP 77 is 10 ms. As indicated by eqautions (15) and (16) the absolute magnitudes of the troughs of the cepstrum of the reflectivity function (Figure 5) at times 10 ms, 20 ms and 30 ms are 0.50, 0.25, and 0.17.

#### Model 2

The reflection coefficients of the lens of model 2 ( Figure 6) are  $R_0=1$  and  $R_1=-3/4$ . At CDP 77 of model 2  $|R_1/R_0|$

MODEL 1  $R_0=1$   $R_1=-1$

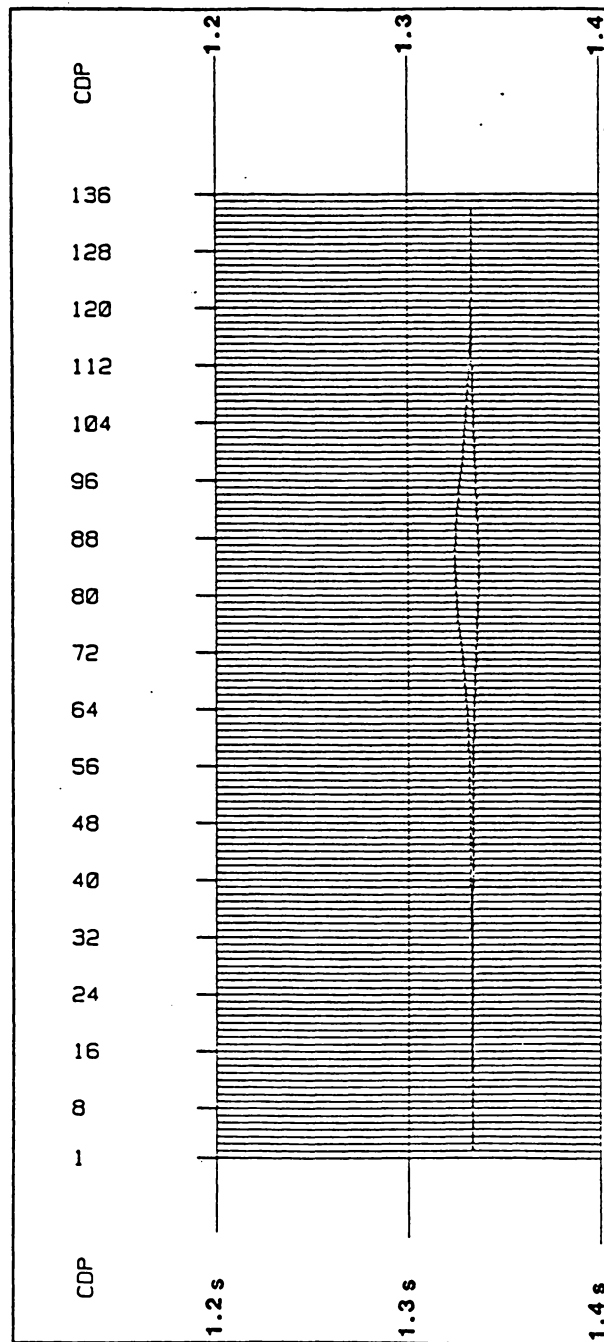


Figure 4. Lens Model 1: The reflection coefficients at the top and bottom of the lens are 1 and -1; respectively. The sample interval is 1/2 ms.

$$R_0=1 \quad R_1=-1 \quad (\text{MODEL 1})$$

TWO-WAY TRAVELTIME OF 10 MS

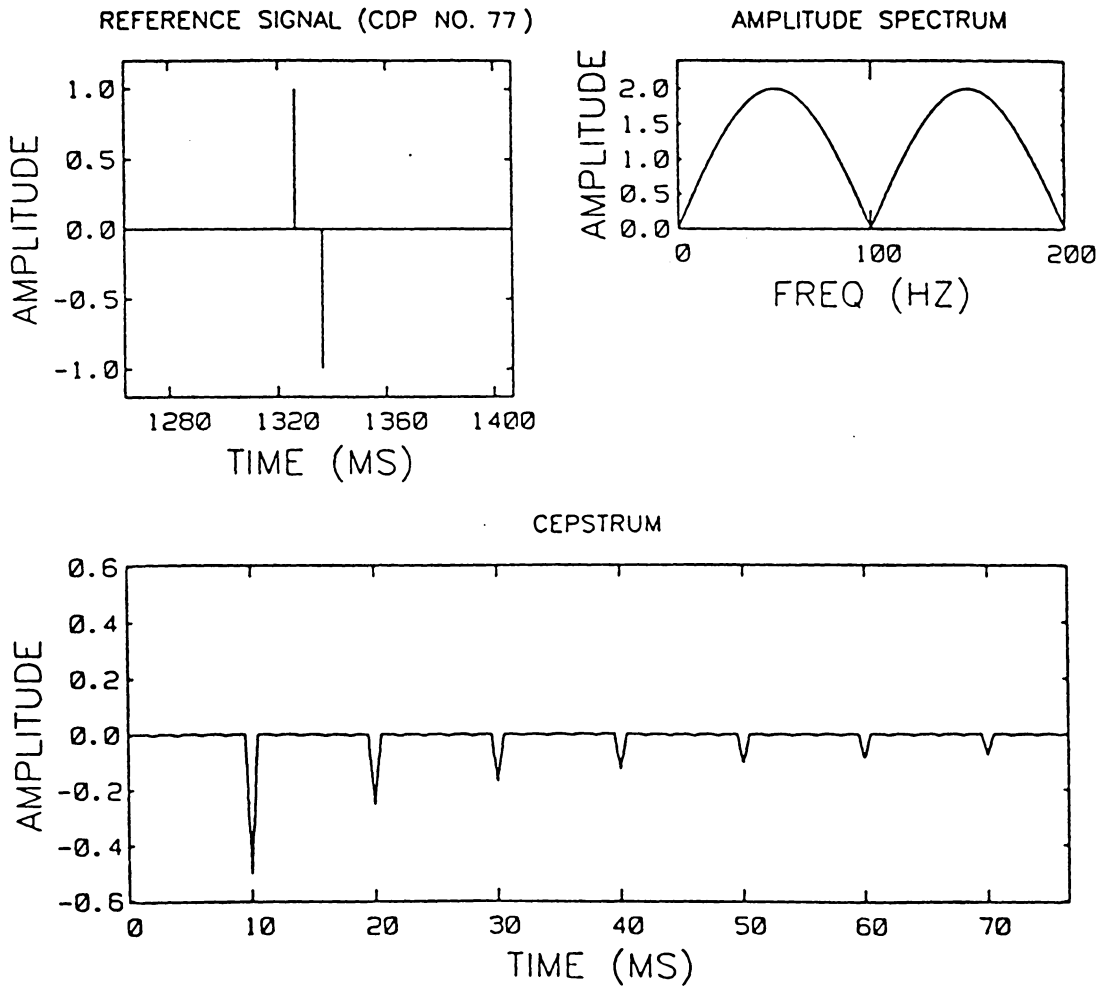


Figure 5.  $|R_1/R_0|=1$ : The cepstrum of the reflectivity function at CDP 77 of model 1. The two-way traveltime is 10 ms and the sample interval is 1/2 ms.

is  $3/4$  (Figure 7) and the two-way traveltime of the lens is 10 ms. Therefore at times 10 ms, 20 ms, and 30 ms the absolute magnitudes of the troughs of the cepstrum of the reflectivity function (Figure 7) are 0.38, 0.14, and 0.07.

### Model 3

The reflection coefficients of the lens of model 3 (Figure 8) are  $R_0=1$  and  $R_1=-1/2$ . At CDP 77 of model 3  $|R_1/R_0|=1/2$  (Figure 9) and the two-way traveltime of the lens is 10 ms. Therefore at times 10 ms, 20ms, and 30 ms the absolute magnitudes of the troughs of the cepstrum of the reflectivity function (Figure 9) are 0.25, 0.063, and 0.021.

### Model 4

The reflection coefficients of model 4 (Figure 10) are  $R_0=1$  and  $R_1=-1/4$ . For the reflection coefficients at CDP 77 of model 4  $|R_1/R_0|=1/4$  (Figure 11) and the two-way traveltime of the lens is 10 ms. Therefore at times 10 ms, 20 ms and 30 ms the absolute magnitudes of the troughs of the cepstrum of the reflectivity function (Figure 11) are absolute magnitudes of 0.13, .016, and 0.0026.

MODEL 2  $R_0=1$   $R_1=-3/4$

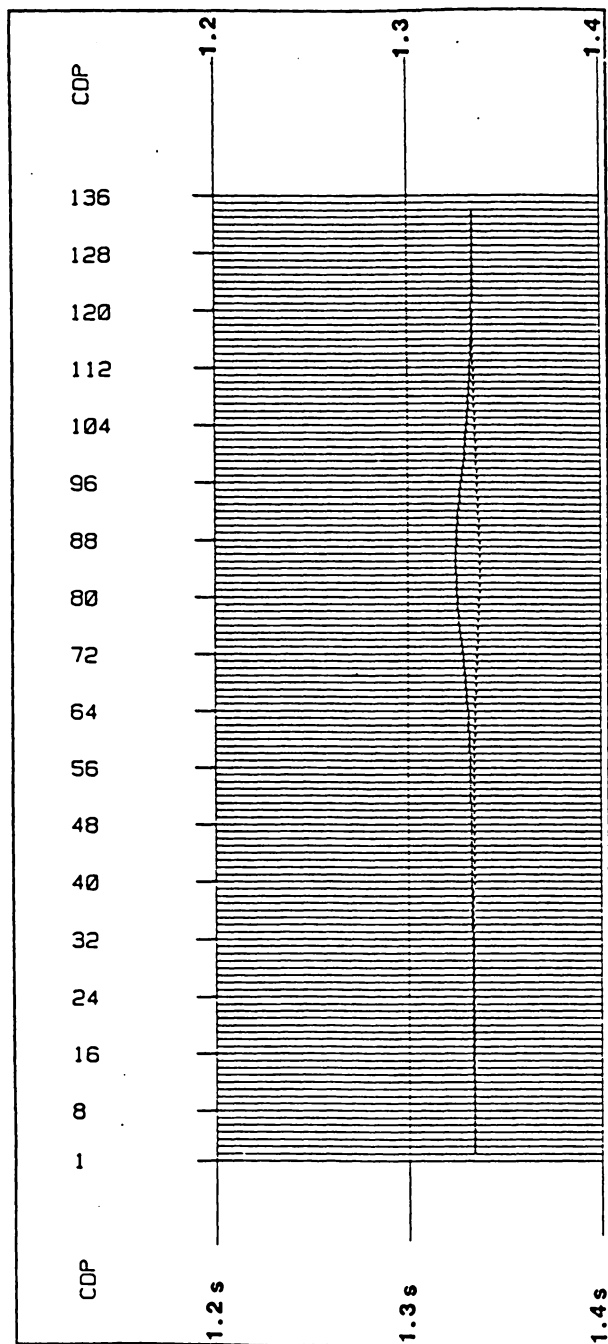


Figure 6. Lens Model 2 : The reflection coefficients at the top and bottom of the lens are 1 and  $-3/4$ ; respectively. The sample interval is  $1/2$  ms.

$$R_0=1 \quad R_1=-3/4 \quad (\text{MODEL 2})$$

TWO-WAY TRAVELTIME OF 10 MS

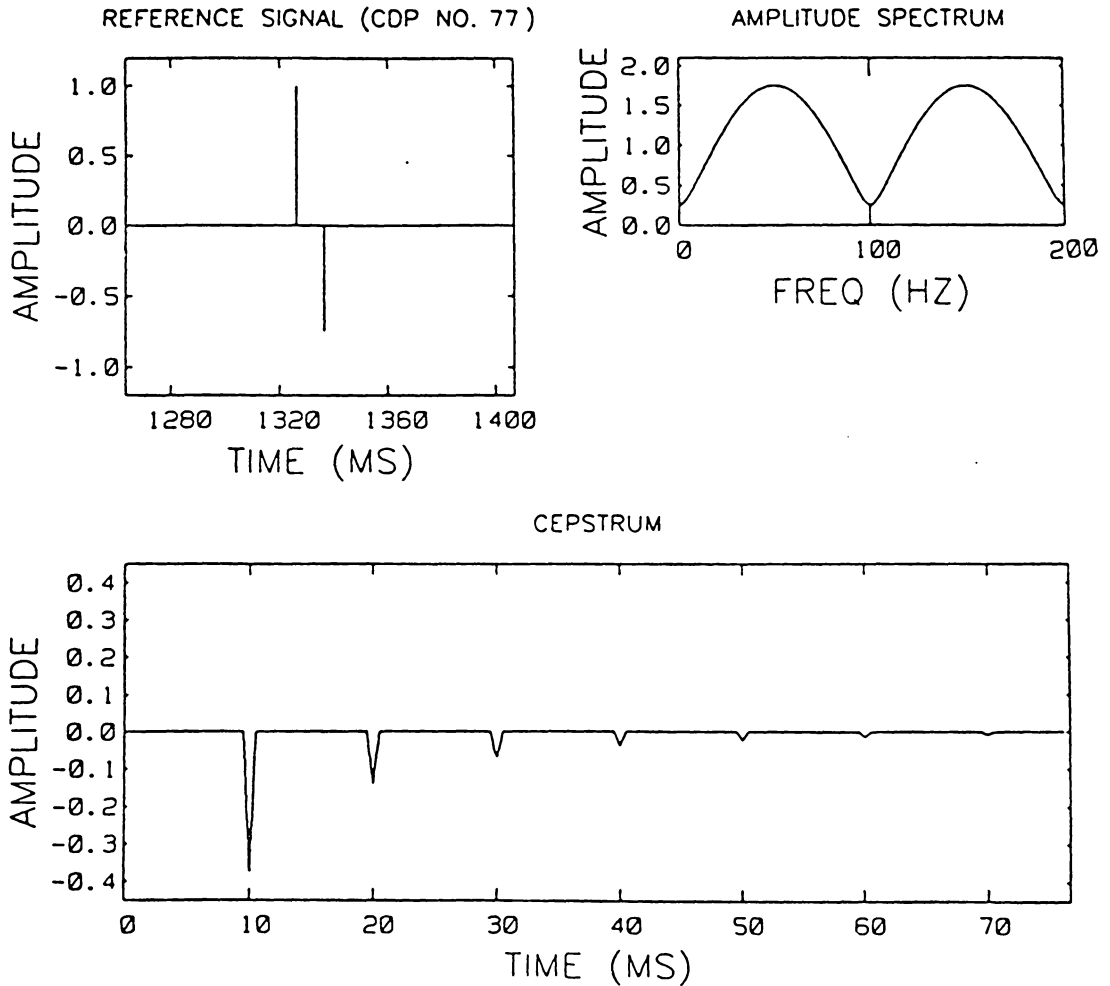


Figure 7.  $|R_1/R_0|=3/4$ : The cepstrum of the reflectivity function at CDP 77 of model 2. The two-way traveltime is 10 ms and the sample interval is 1/2 ms.

MODEL 3  $R_0=1$   $R_1=-1/2$

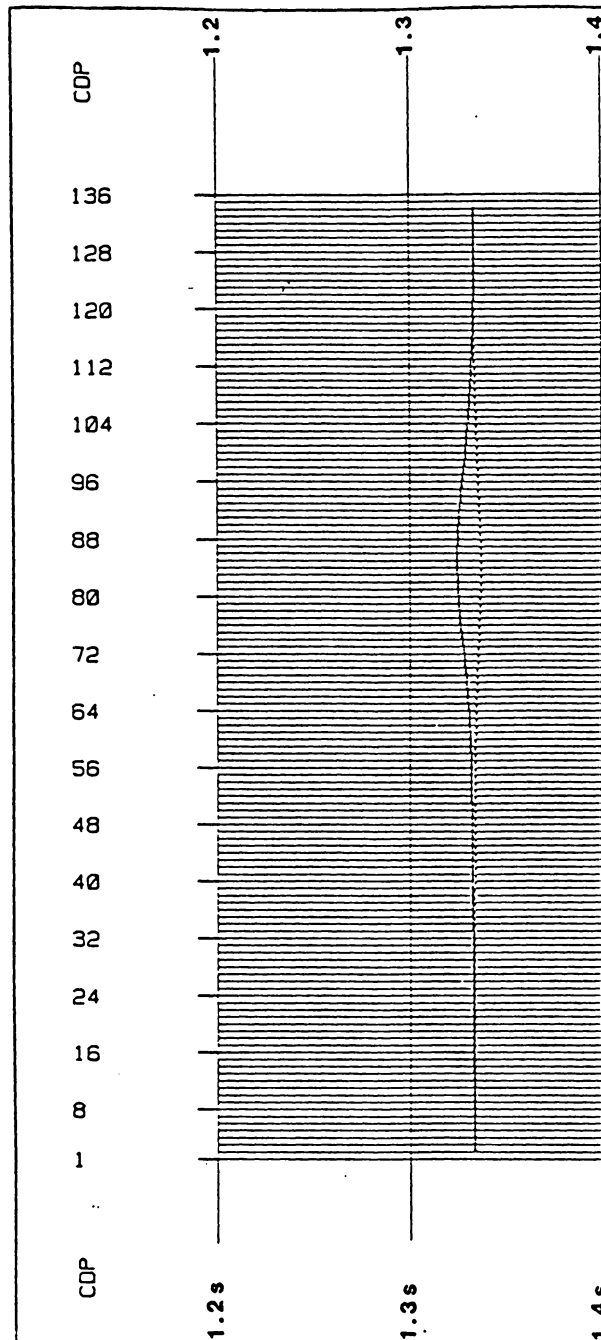


Figure 8. Lens Model 3 : The reflection coefficient at the top and bottom of the lens are 1 and  $-1/2$ ; respectively. The sample rate is  $1/2$  ms.

$$R_0 = 1 \quad R_1 = -1/2 \quad (\text{MODEL 3})$$

TWO-WAY TRAVELTIME OF 10 MS

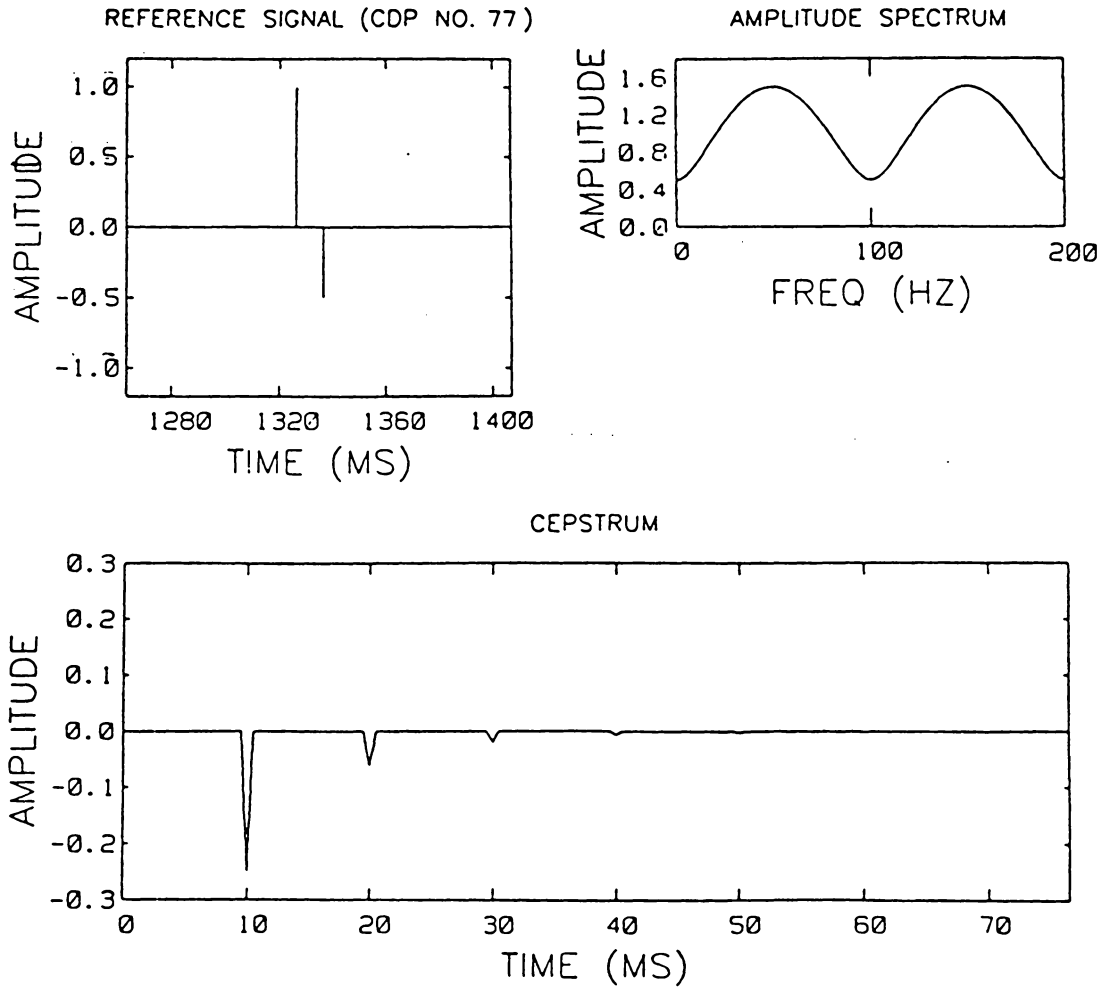


Figure 9.  $|R_1/R_0|=1/2$ : The cepstrum of the reflectivity function at CDP 77 of model 3. The two-way traveltime is 10 ms and the sample interval is 1/2 ms.

MODEL 4  $R_0 = 1$   $R_1 = -1/4$

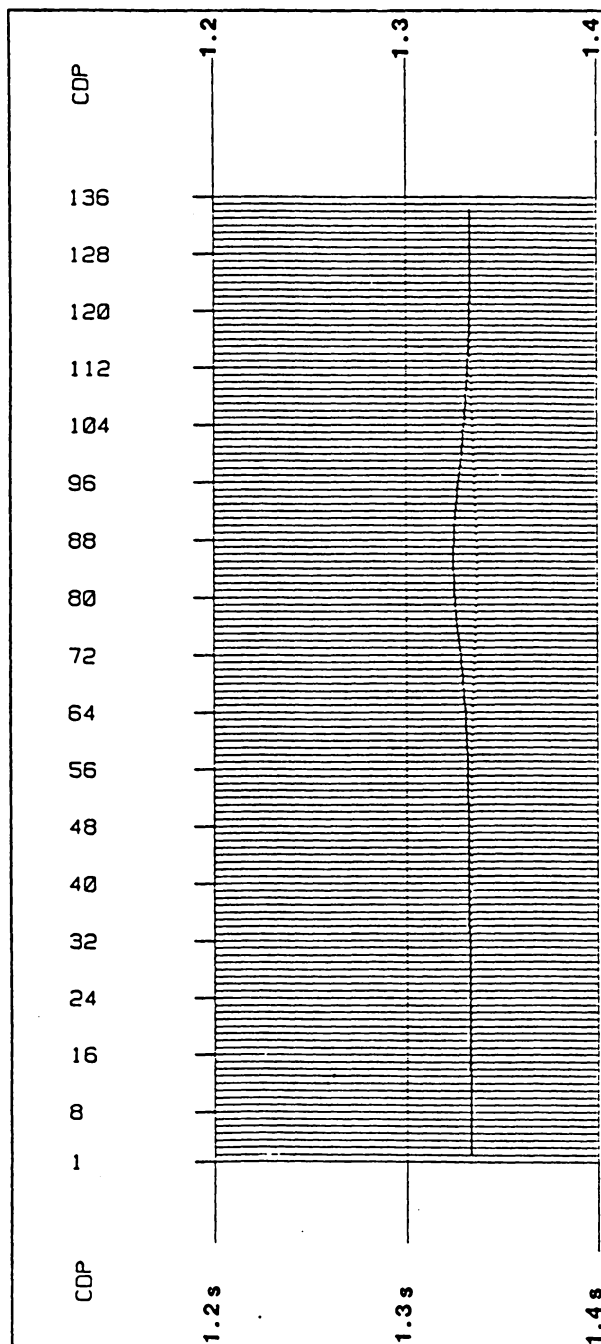


Figure 10. Lens Model 4 : The reflection coefficient at the top and bottom of the lens are 1. and  $-1/4$ ; respectively. The sample interval is  $1/2$  ms.

$$R_0=1 \quad R_1=-1/4 \quad (\text{MODEL 4})$$

TWO-WAY TRAVELTIME OF 10 MS

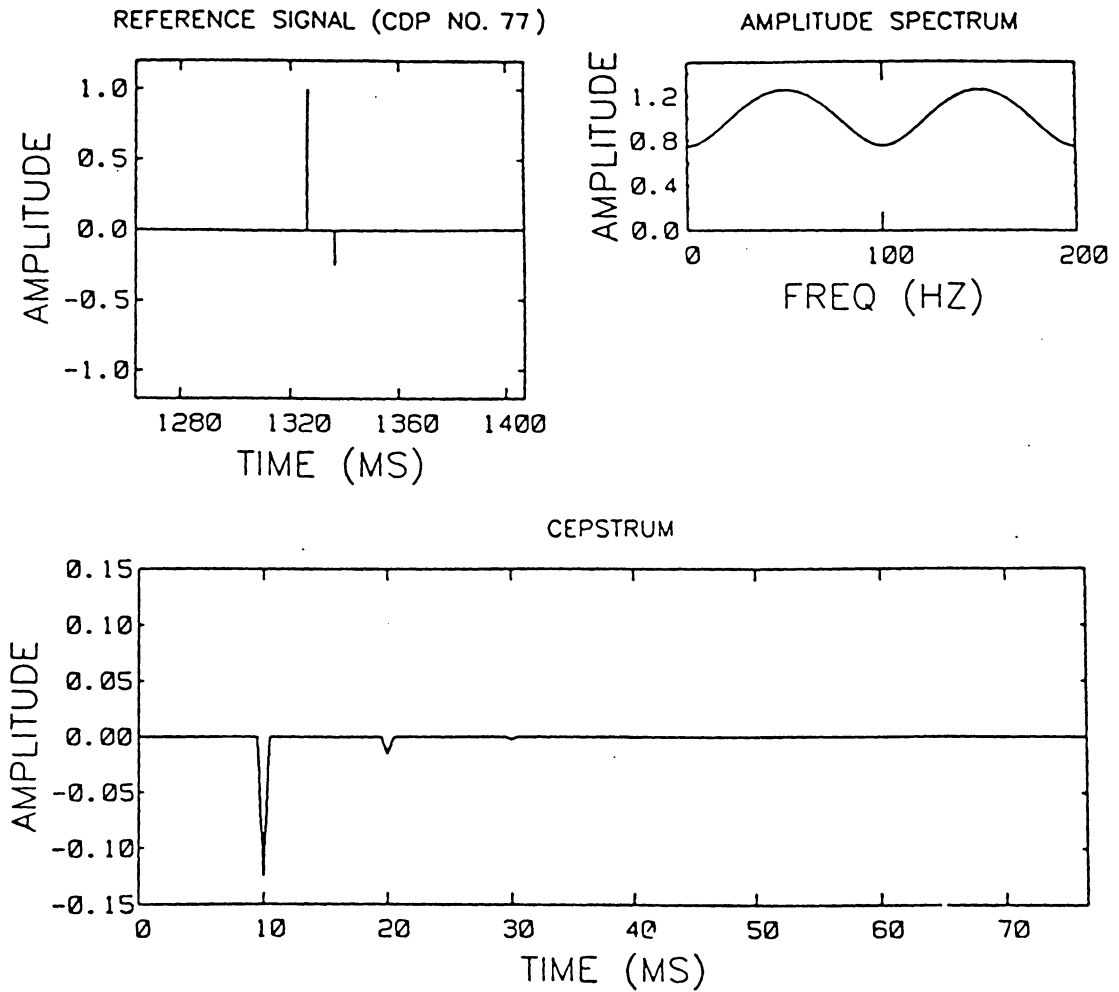


Figure 11.  $|R_1/R_0|=1/4$ : The cepstrum of the reflectivity function at CDP 77 of model 4. The two-way traveltime is 10 ms and the sample interval is 1/2 ms.

### Comparison of the cepstra of Models 1 to 4

Observation of the cepstra of the reflectivity functions at CDP 77 of models 1 to 4 reveals a reduction in the absolute magnitudes of the troughs of the cepstrum as  $|R_1/R_0|$  decreases. For instance, whereas the first cepstral trough is -0.5 when  $|R_0/R_1|=1$  (Figure 5) the first cepstral trough is -0.13 when  $|R_1/R_0|=1/4$  (Figure 11). In addition, as  $|R_1/R_0|$  decreases, the rate of the decay of the absolute magnitudes of the troughs of any given cepstrum increases. Therefore resolution in the frequency domain diminishes as  $|R_1/R_0|$  decreases. Optimum resolution is achieved when  $|R_1/R_0|=1$

### **The effects of reversing the order of the reflection coefficients.**

Although changing the ratios of the reflection coefficients changes the resolution in the frequency domain, reversing the reflection coefficients does not change the cepstrum or its related functions. The reflectivity function at CDP 77 of model 5 is used to illustrate this point (Figure 13). A sample interval of 1/2 ms was used to generate model 5. The reflection coefficients of the lens of model 5 are  $R_0=-1/4$  and  $R_1=1$ ; for instance, the model contains a low speed lens. The reflection coefficients of model 5 occur in the reverse order of those of model 4. (Figure 11). However, by referring to Figure 11 and Figure 13, it becomes clear that there is no difference between the cepstra of the two reflectivity functions.

MODEL 5  $R_0 = -1/4$   $R_1 = 1$

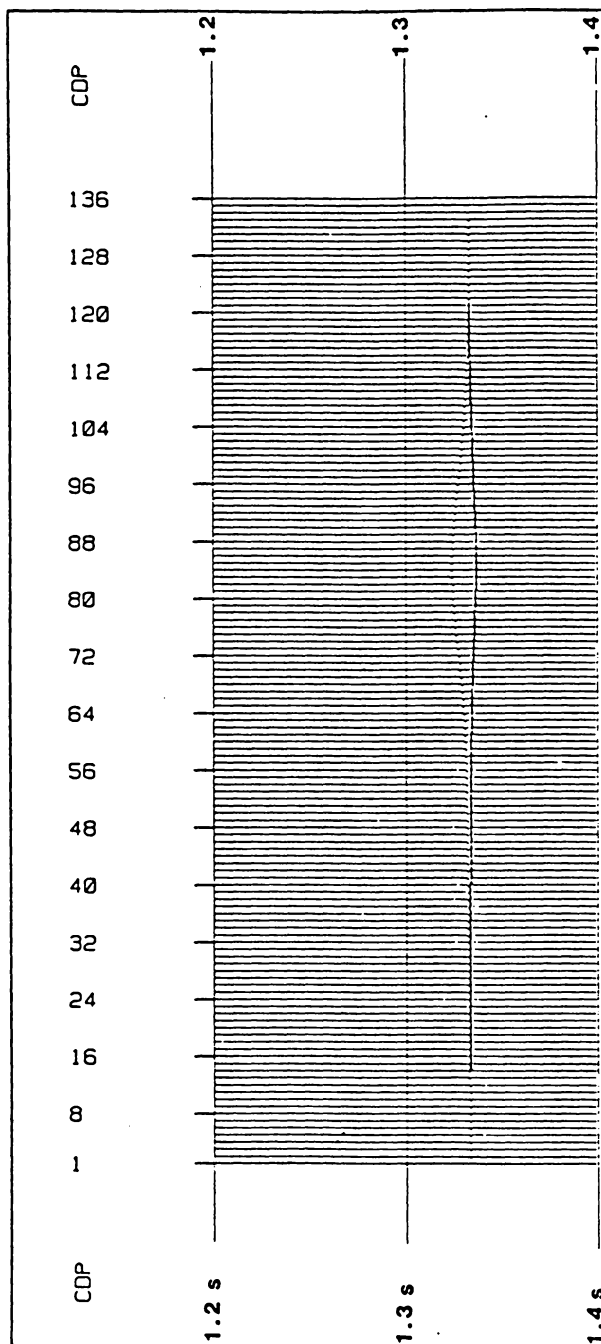
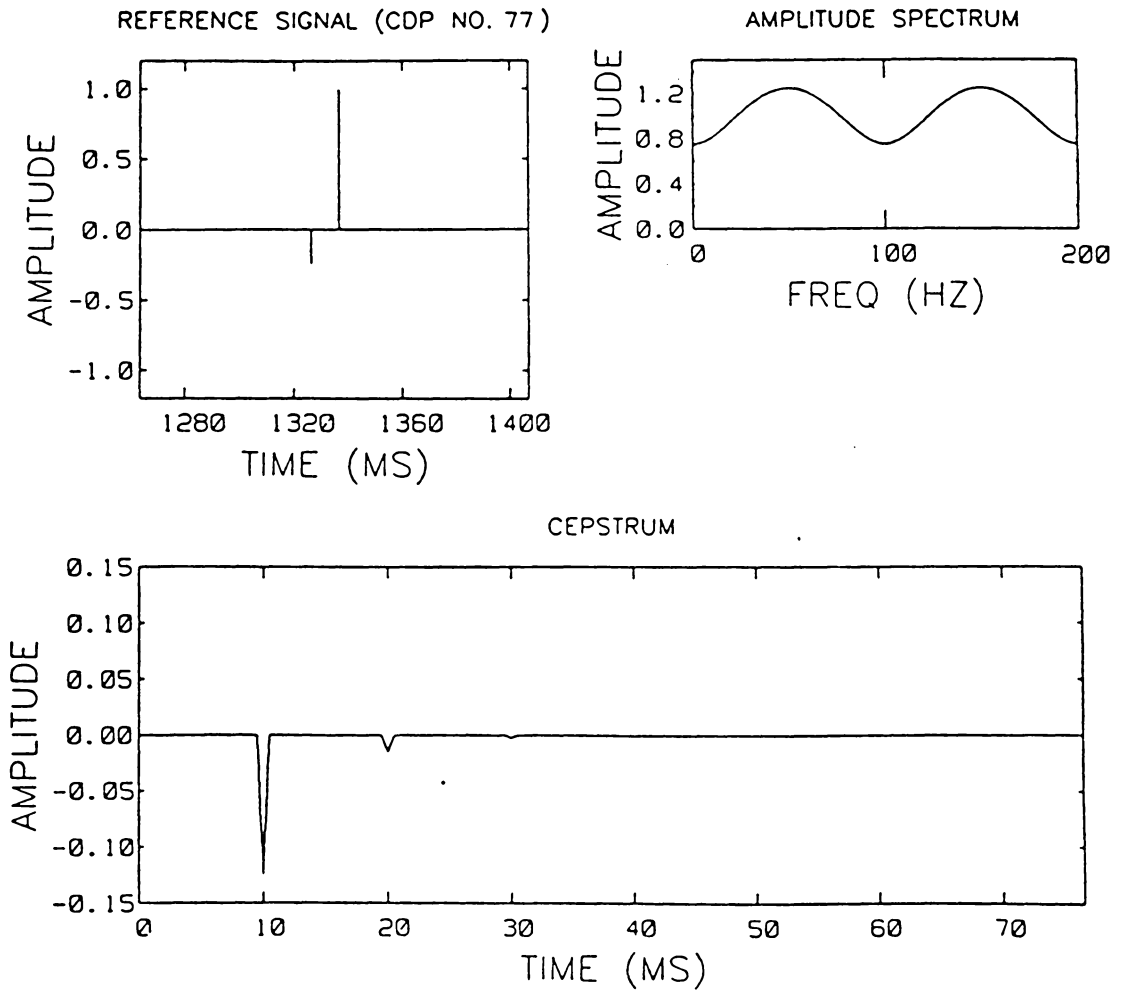


Figure 12. Lens Model 5 : The reflection coefficient at the top and bottom of the lens are  $-1/4$  and  $1$ ; respectively. The sample interval is  $1/2$  ms.

Figure 13. Reflectivity function of model 5: The reflectivity function at CDP 77 of model 5 is shown. The reflection coefficients of the reflectivity function are in the reverse order of those of the reflectivity function at CDP 77 of model 4 (Figure 11); in every other aspect the two reflectivity functions are identical. Although the reflection coefficients are reversed, the cepstra of both reflectivity functions are identical.

$$R_0 = -1/4 \quad R_1 = 1 \quad (\text{MODEL 5})$$

TWO-WAY TRAVELTIME OF 10 MS



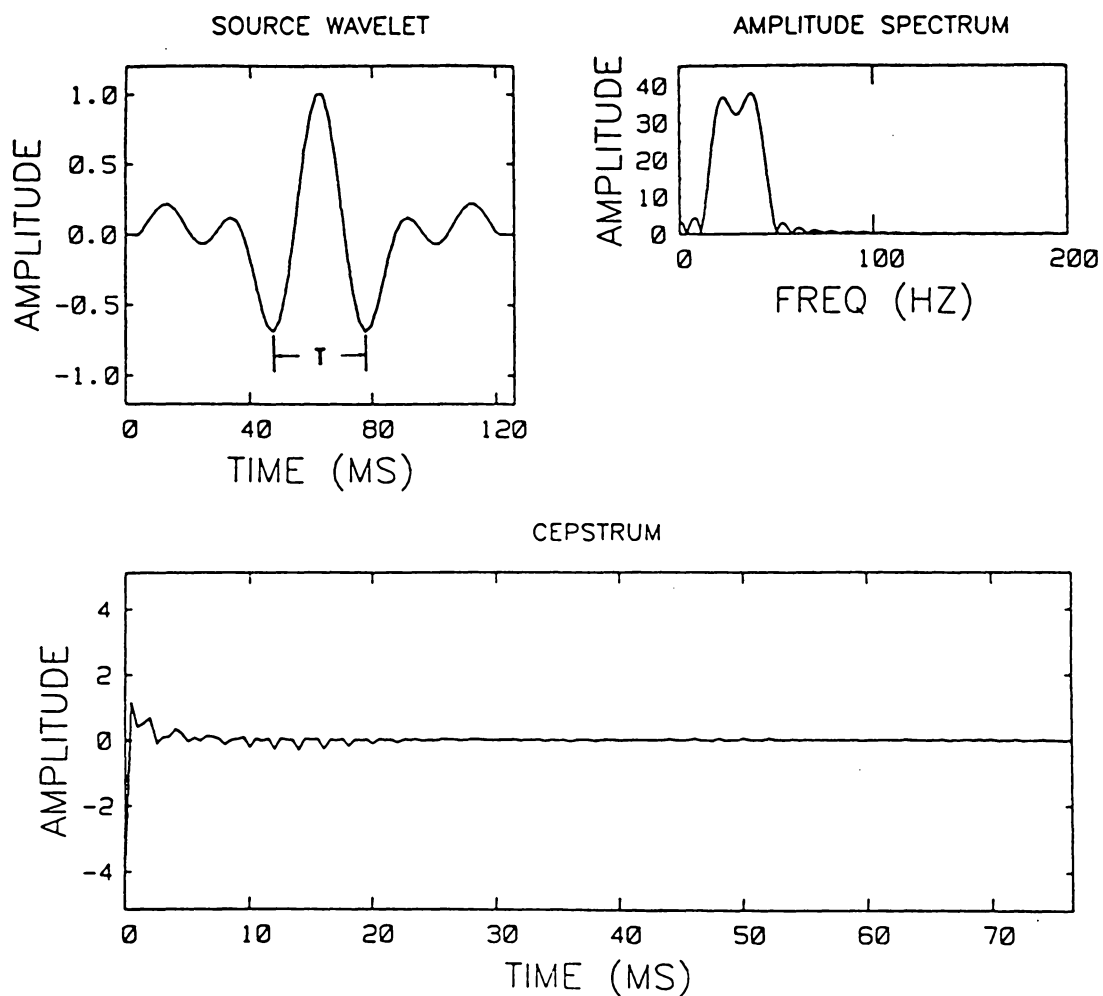


Figure 14. Source wavelet: The Klauder wavelet used to generate reflections from the lens of model 1 is shown. The basic period,  $T$ , of the wavelet is 33 ms and the amplitude spectrum is bandlimited between 15 Hz and 45 Hz. The cepstrum of the Klauder wavelet is also shown. The wavelet is sampled every 1/2 ms.

## The source wavelet

A tapered Klauder wavelet ( Figure 14), sampled every 1/2 ms, was convolved with the reflectivity functions of model 1 (Figure 4) to create reflections from the thin lens (model 6 (Figure 15) contains the reflections from the lens of model 1). The Klauder wavelet is bandlimited between 15 HZ and 45 HZ and has a basic period of 33 ms, as measured from trough to trough (Figure 14). The cepstrum of the Klauder wavelet is irregular and conceals the pulses of the cepstra of the reflectivity functions of the lens. However as is shown below, by computing the sub-cepstrum and sum-cepstrum the effects of the cepstrum of the wavelet are eliminated.

## The sub-cepstrum, sum-cepstrum and discriminator

To show that the cepstrum of the source wavelet can be removed from the cepstrum of the reflection, the sub-cepstrum of the reflections at CDP 77 and CDP 60 (Figure 16) of model 6 is shown in Figure 17. The reflectivity functions at CDP's 60 and 77 of model 1 are shown in (Figure 18). The sub-cepstrum of the reflectivity functions are shown in Figure 19. The sub-cepstrum of the reflections is identical to the sub-cepstrum of the reflectivity functions. Therefore, subtraction in the quefreny domain has eliminated the cepstrum of the source wavelet.

The two-way travelttime at CDP's 60 and 77 are 2.5 ms and 10 ms; respectively. The two-way travelttime of 2.5 ms is

MODEL 6 CONVOLUTION OF SOURCE WITH MODEL 1

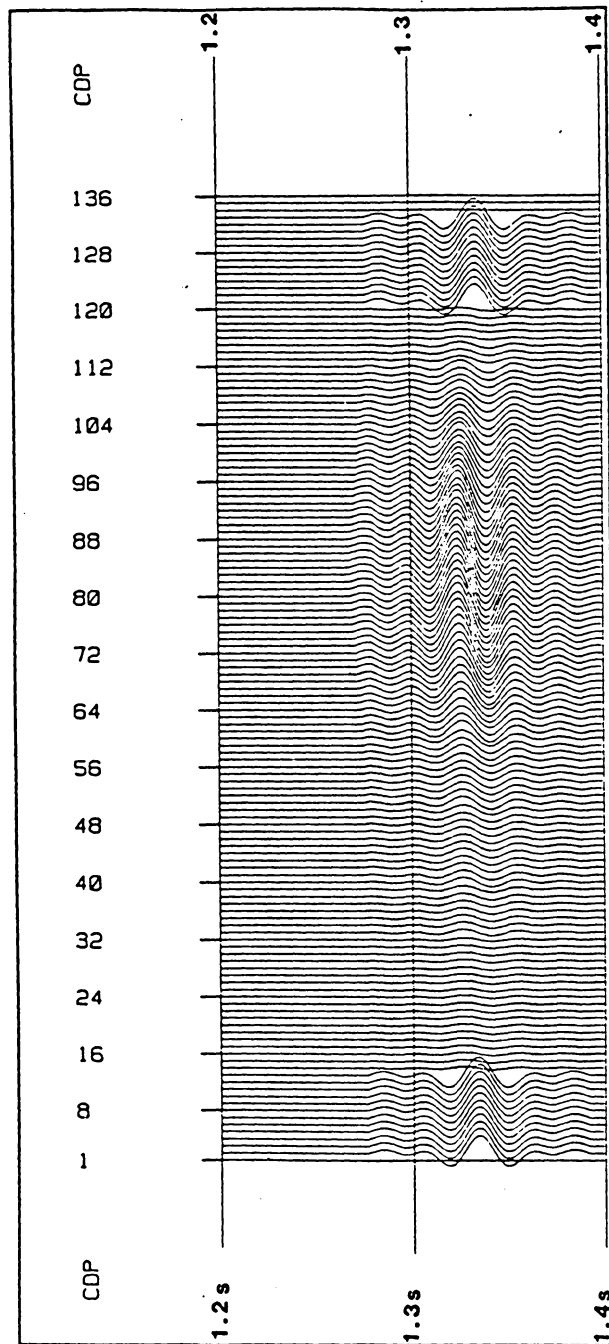


Figure 15. Lens Model 6: The reflections from the lens of model 1. The sample interval is 1/2 ms.

## REFLECTIONS OF MODEL 6

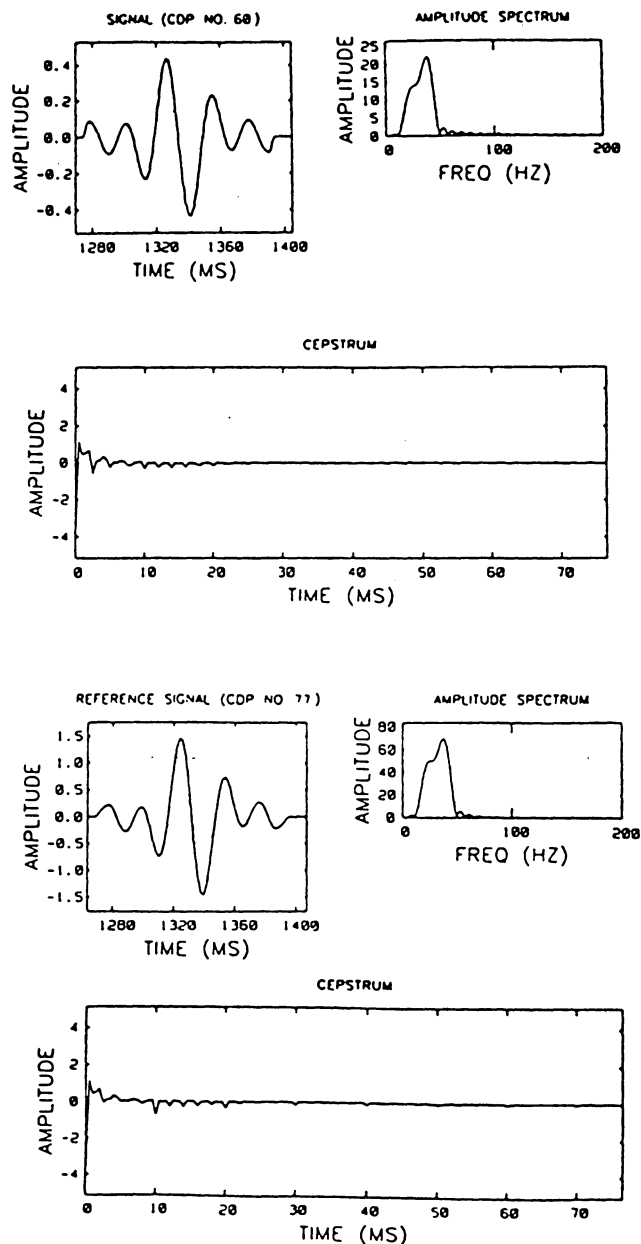


Figure 16. Reflections at CDP's 60 and 77 : The reflections at CDP's 60 and 77 of model 6 are shown. The cepstra of the reflections are also shown. The two-way traveltime at CDP 60 is 2.5 ms and the two-way traveltime at CDP 77 is 10 ms. The sample interval is 1/2 ms.

## ANALYTIC FUNCTIONS OF REFLECTIONS

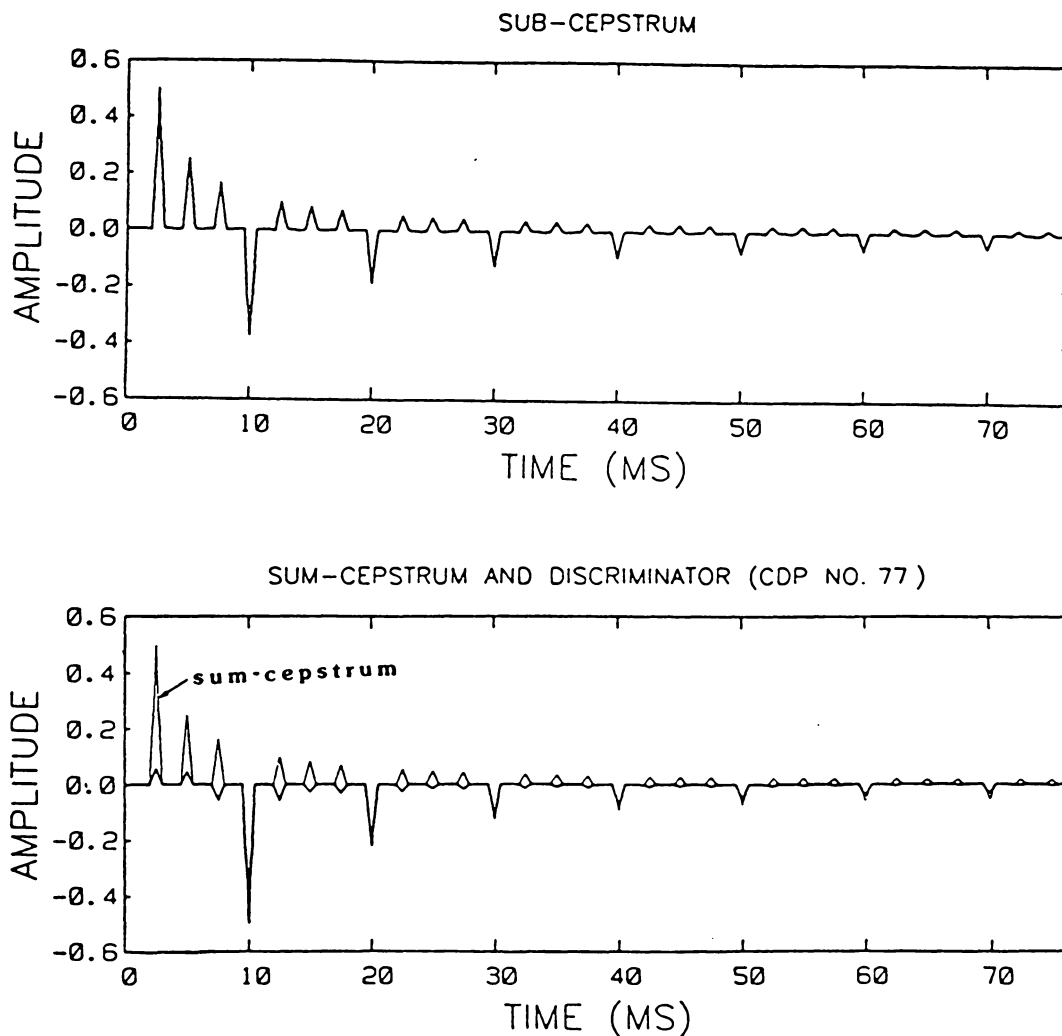


Figure 17. Analytic functions of reflections: The sub-cepstrum, sum-cepstrum and discriminator (dark line) of reflection at CDP's 60 (two-way traveltime of 2.5 ms) and 77 (two-way traveltime of 10 ms) of model 6 are depicted. The discriminator has amplified the troughs occurring every 10 ms. In this and subsequent figures, the discriminator has been normalized such that its maximum amplitude equals the maximum amplitude of the sum-cepstrum.

### REFLECTIVITY FUNCTIONS OF MODEL 1

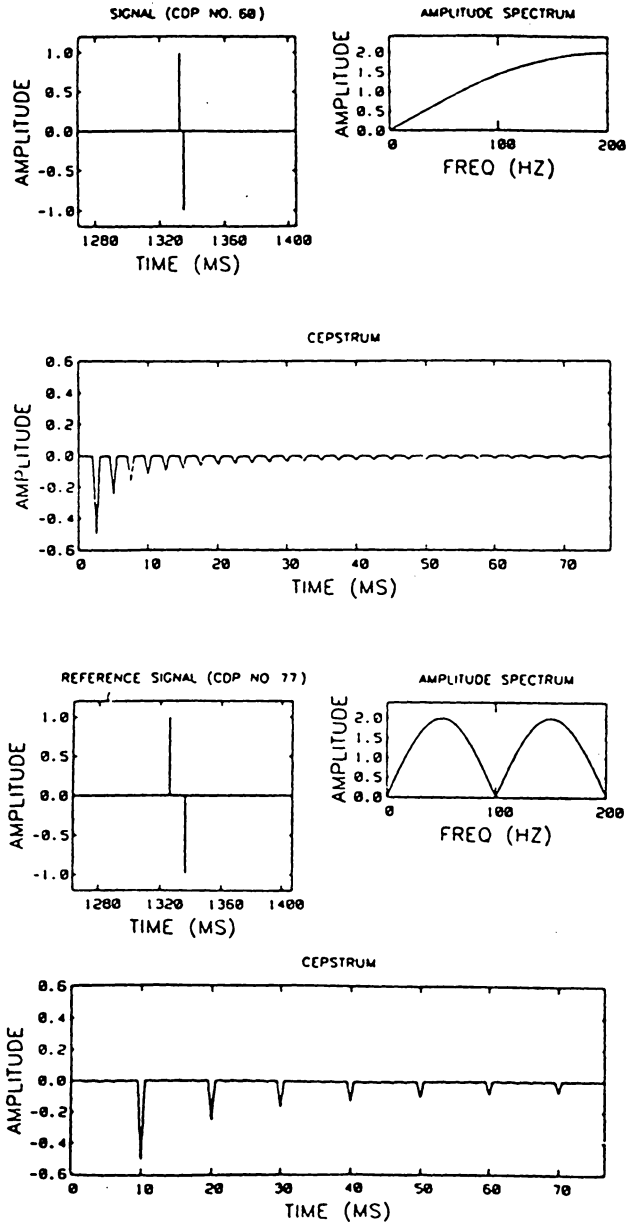


Figure 18. Reflectivity functions at CDP's 60 and 77: The reflectivity functions at CDP's 60 (two-way traveltime of 2.5 ms) and 70 (two-way traveltime of 10 ms) of model 1 are shown. The cepstrum of each function is also displayed.

## SUB-CEPSTRUM OF REFLECTIVITY FUNCTIONS

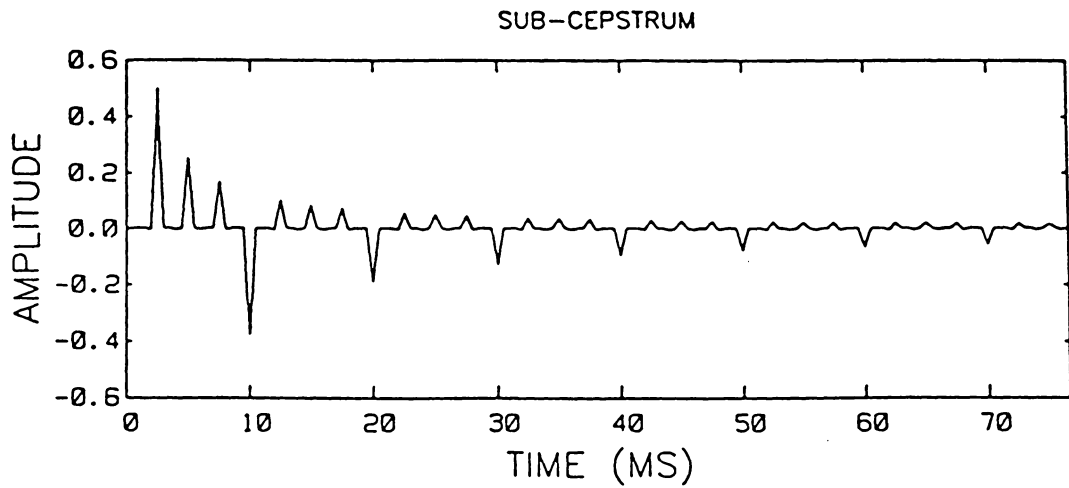


Figure 19. Sub-cepstrum of reflectivity functions: The sub-cepstrum of the reflectivity functions at CDP's 60 and 77 (Figure 18) of model 1 are shown.

equal to the interval separating the peaks of the sub-cepstrum and sum-cepstrum (Figure 17); the traveltime of 10 ms is equal to the period between the troughs of the same functions. Significantly, neither period is as conspicuous in the cepstrum of the reflection at either CDP (Figure 16) because the cepstrum of the source wavelet has masked the cepstral pulses of the reflectivity functions.

The effectiveness of the discriminator is demonstrated in Figure 17. For instance, the discriminator has amplified the periodic troughs relative to all other amplitudes of the sum-cepstrum, thereby correctly highlighting the 10 ms period of the troughs of the sum-cepstrum. The correct period of the sum-cepstrum is not 2.5 ms. Although within each trio of peaks of the sum-cepstrum, there is a period of 2.5 ms, a fourth peak is missing at each interval of 10 ms.

#### **The effects of the sample interval**

In cepstrum analysis, the sample interval affects resolution. For example, by equations (15) and (16), the minimum two-way traveltime (thin-bed thickness) that can be detected with multiple pulses of the cepstrum is two sample intervals. In addition it is shown that the sample interval affects the shape of cepstral pulses. Reflections at CDP 55 and CDP 77 of model 6 (Figure 15) are used to illustrate these facts.

At CDP 55 the lens has a two-way traveltime of 2 ms. This two-way traveltime is confirmed by the 2 ms period between troughs of the sum-cepstrum and discriminator of the reflection at CDP 55 of model 6, which are shown in Figure 20. The period of 2 ms is evident between times  $t=0$  ms and  $t=16$  ms. The sum-cepstrum and discriminator were computed by using the reflections at CDP's 60 through 75.

To demonstrate the importance of the sample interval, the thin lens (Figure 3) was sampled every 1 ms and the Klauder wavelet, also sampled every 1 ms, convolved with the reflectivity functions. As with model 1, the reflection coefficients at the top and bottom of the lens are 1 and -1, respectively. The sum-cepstrum and discriminator (Figure 21) of the reflection at CDP 55 were computed as above. Because the sample interval was increased, the troughs of the sum-cepstrum broadened (Figure 21) and can only be traced between times 0 ms and 10 ms. In the discriminator, periodic troughs occurs only at 2 ms and 4 ms. Effectively, the increased sample interval has reduced the resolution by broadening the periodic troughs and reducing the number of distinctive periodic troughs.

Next, the thin lens (Figure 3) was sampled with a sample interval of 2 ms and the reflections generated with the Klauder wavelet, which was also sampled at 2 ms. Reflection coefficients at the top and bottom of the lens were also 1 and -1. The test was repeated for the reflection at CDP 55

Figure 20. Reflection at CDP 55 of Model 6: The reference signal is the reflection at CDP 55 of model 6. The sample interval is 1/2 ms. the sum-cepstrum is based on reflections at CDP's 60 to 75. At CDP 55 the two-way traveltime of the lens is 2 ms. The 2 ms traveltime is resolved in the sum-cepstrum and discriminator as a period of 2 ms between troughs.

SAMPLE INTERVAL OF 1/2 MS  
TWO-WAY TRAVELTIME OF 2 MS  
SUM-CEPSTRUM BASED ON CDP'S 60-75

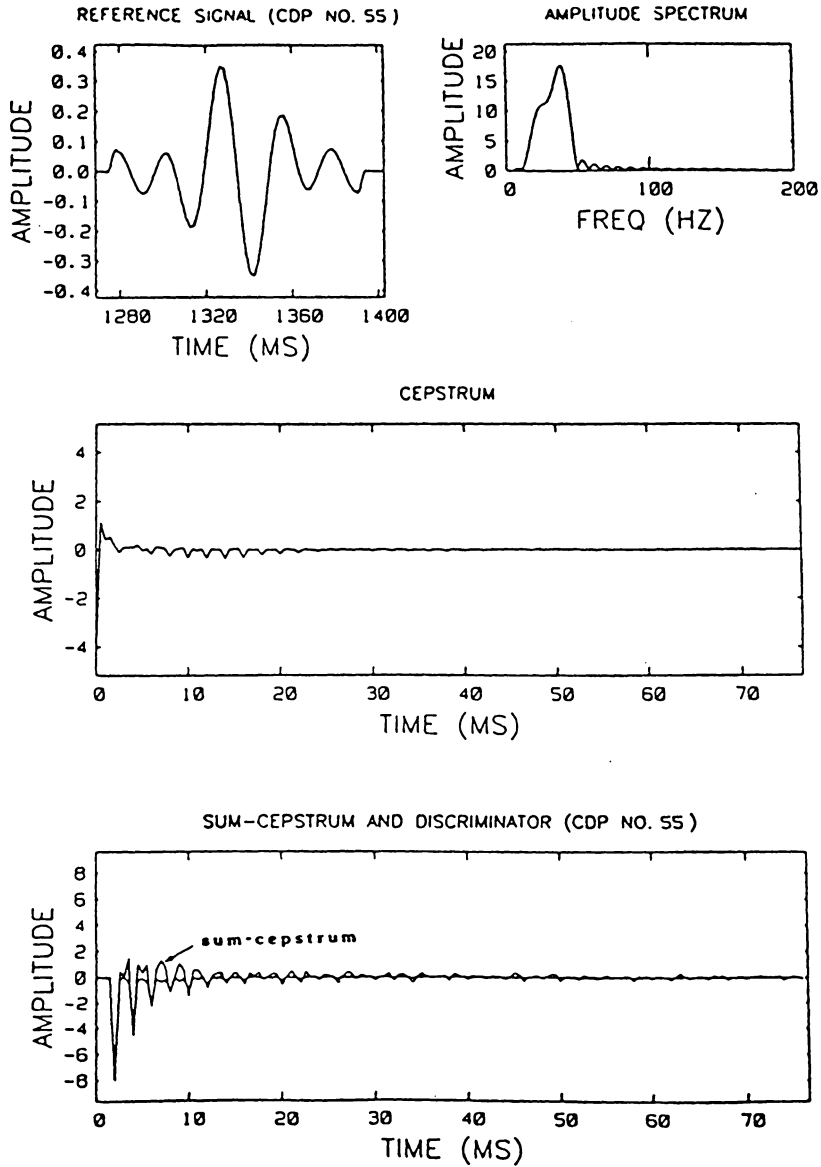


Figure 21. Reflection at CDP 55 ( $dt=1$  ms) : The reference signal is the reflection at CDP 55. The new sample interval is 1 ms. The sum-cepstrum is based on reflections at CDP's 60 to 75. Increasing the sample interval from  $1/2$  ms (Figure 20) to 1 ms has reduced resolution in the quefreny domain by broadening the periodic troughs and reducing the number of visible periodic troughs.

SAMPLE INTERVAL OF 1 MS

TWO-WAY TRAVELTIME OF 2 MS

SUM-CEPSTRUM BASED ON CDP'S 60-75

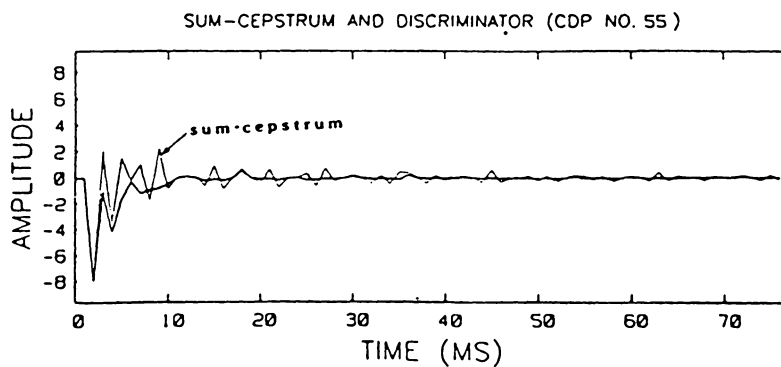
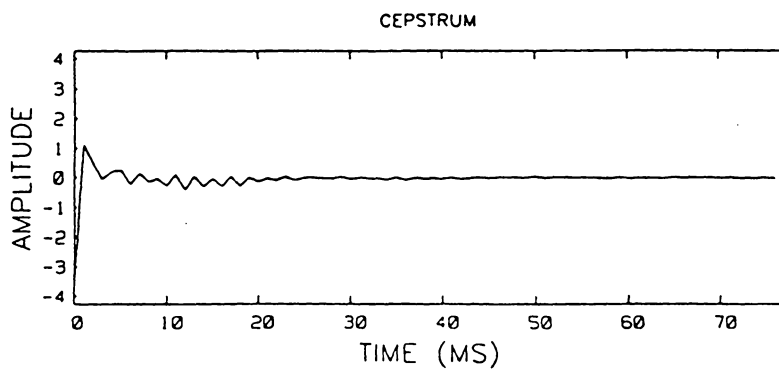
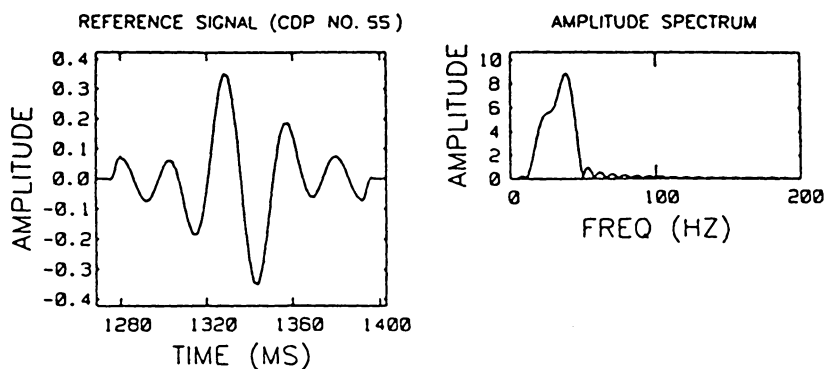
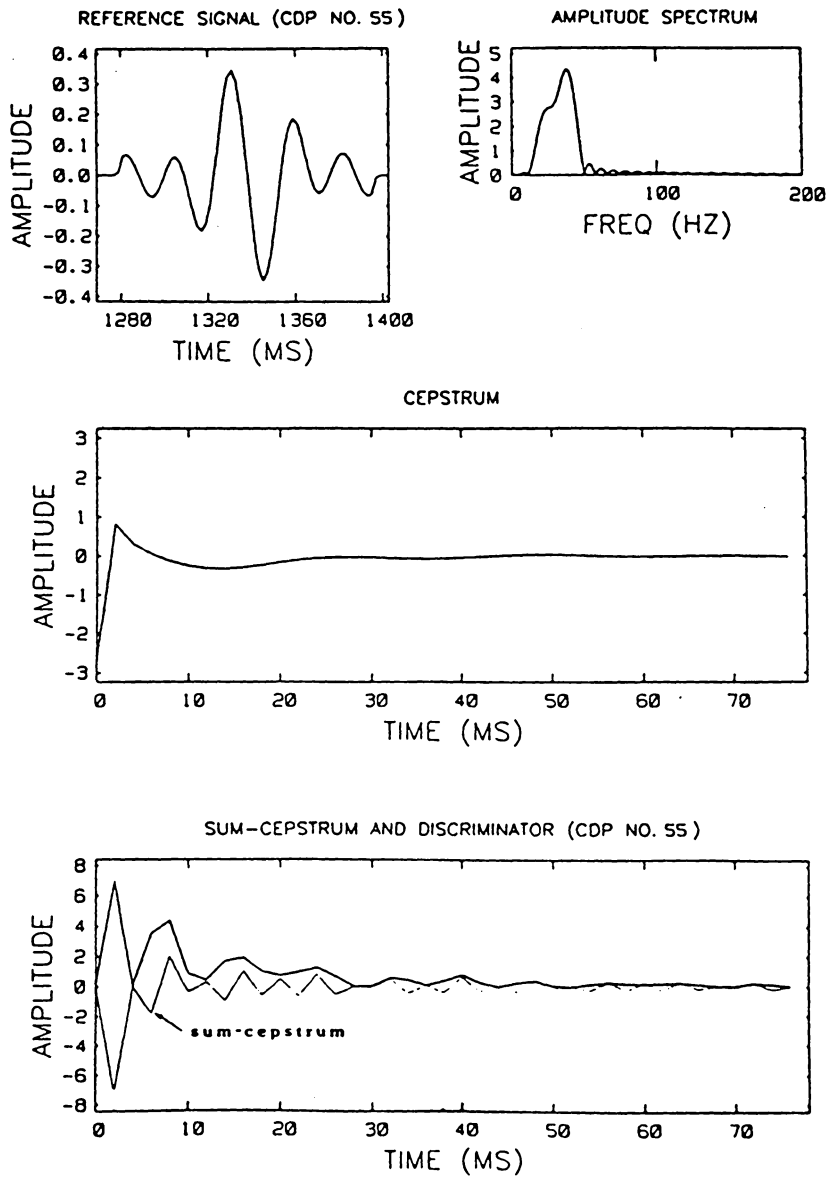


Figure 22. Reflection at CDP 55 ( $dt=2$  ms): The reference signal is the reflection at CDP 55. The new sample interval is 2 ms. The sum-cepstrum is based on reflections at CDP's 60 to 75. The 2 ms traveltime is not resolved in the sum-cepstrum nor the discriminator because the sample interval is too large.

SAMPLE INTERVAL OF 2 MS

TWO-WAY TRAVELTIME OF 2 MS

SUM-CEPSTRUM BASED ON CDP'S 60-75



(Figure 22). The two-way traveltime of 2 ms cannot be distinguished in either the sum-cepstrum or the discriminator when the sample interval is 2 ms. Although there is a trough in the sum-cepstrum at 2 ms, no periodic troughs occur. The sample interval of 2 ms is too large for the detection of layers with two-way traveltimes of 2 ms or less.

The effects of the sample interval were investigated further by using the reflectivity function at CDP 77 of model 6 as the reference signal. At CDP 77 the lens has a two-way traveltime of 10 ms, therefore the sample intervals of 1/2 ms, 1 ms and 2 ms are small enough for detection of the two-way traveltime. The tests were repeated with sample intervals of 1ms and 2 ms. Figure 23 through Figure 25 show the results obtained for the different sample intervals.

For each test the correct two-way traveltime of 10 ms has been resolved. However, the resolution decreases as the sample interval increases. Troughs of the sum-cepstrum and discriminator broadened as the sample interval increased. In short, the finest sample interval produced the best resolution in the quefreny domain.

#### **The effects of random noise**

The effects of random noise on resolution in the quefreny domain was studied by analyzing reflections to

Figure 23. Reflection at CDP 77 of model 6: The reflection at CDP 77 is the reference signal. The sample interval is 1/2 ms. The sum-cepstrum is based on reflections at CDP's 60 to 75. The two-way traveltime at CDP 77 is 10 ms. The two-way traveltime is resolved in the sum-cepstrum and discriminator as a period of 10 ms between troughs.

SAMPLE INTERVAL OF 1/2 MS

TWO-WAY TRAVELTIME OF 10 MS

SUM-CEPSTRUM BASED ON CDP'S 60-75

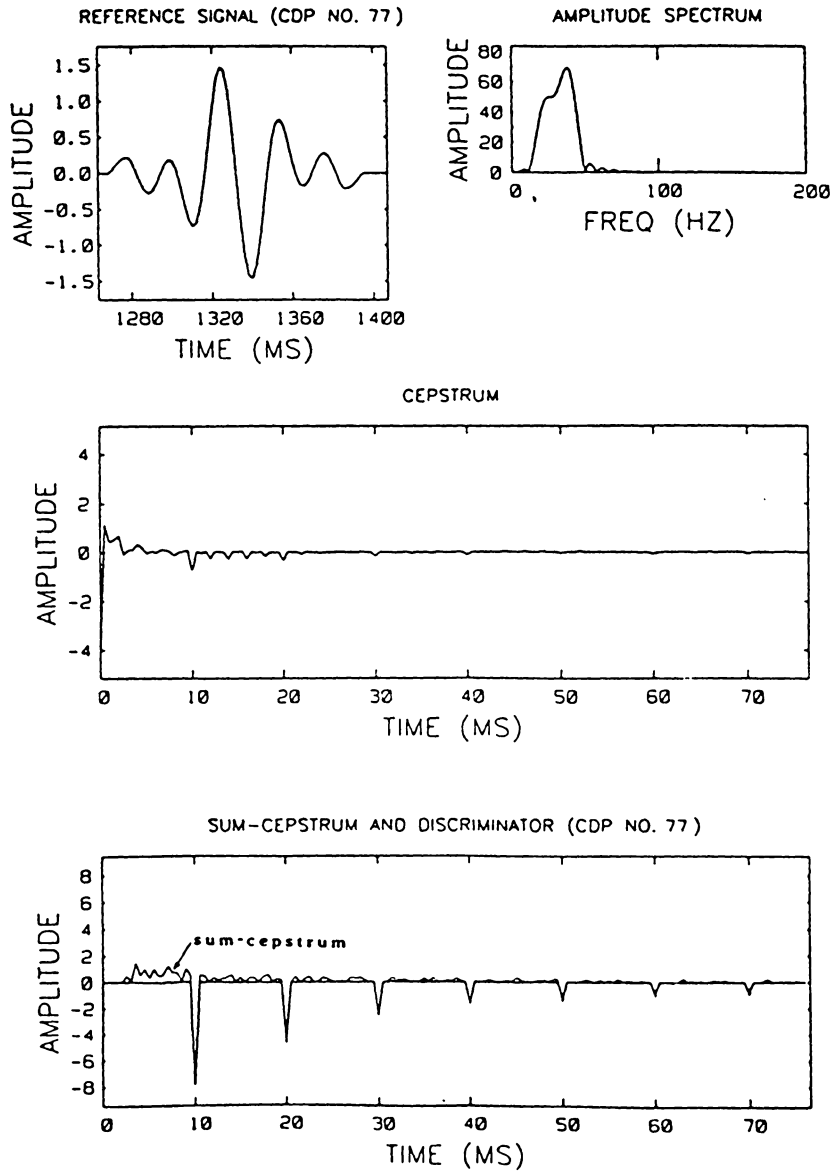


Figure 24. Reflection at CDP 77 ( $dt=1$  ms): The reference signal is the reflection at CDP 77. The sample interval is 1 ms. The sum-cepstrum is based on reflections at CDP's 60 to 75. A comparison of the sum-cepstrum and discriminator of Figure 23 shows that the larger sample interval of 1 ms has broadened the troughs of the sum-cepstrum and discriminator.

SAMPLE INTERVAL OF 1 MS

TWO-WAY TRAVELTIME OF 10 MS

SUM-CEPSTRUM BASED ON CDP'S 60-75

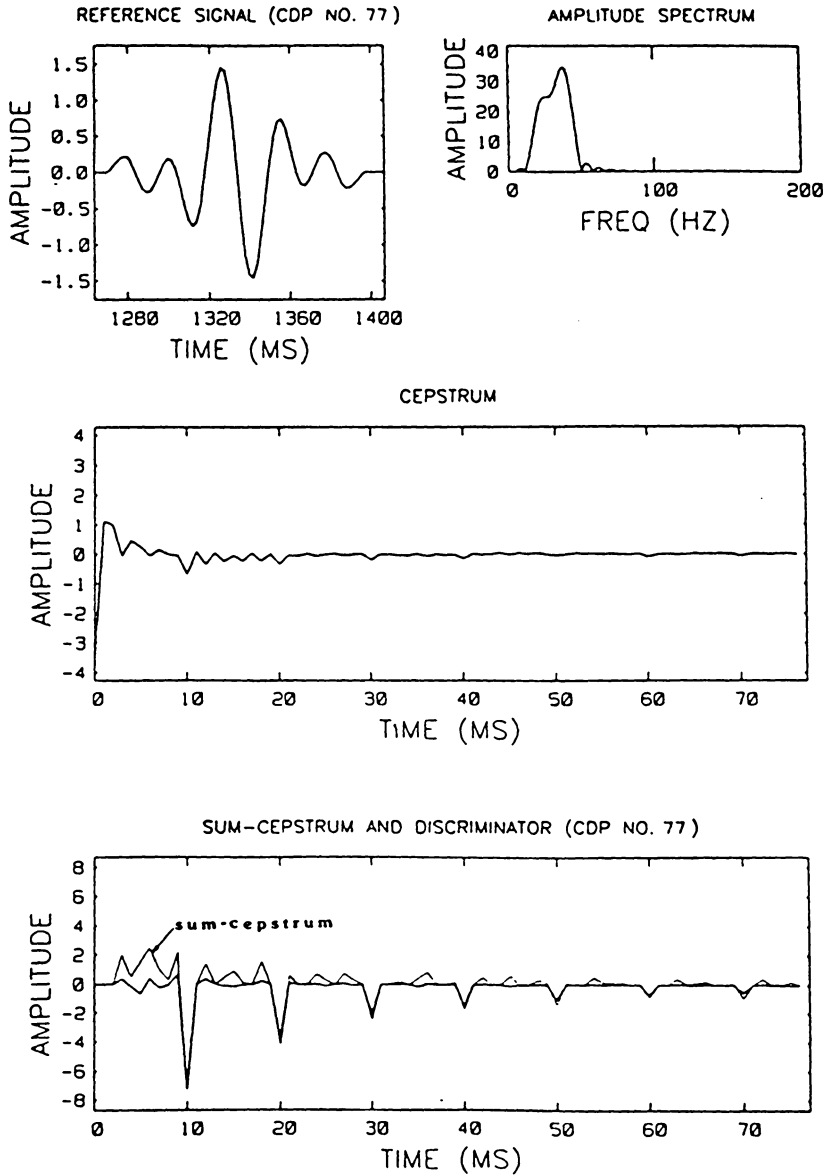
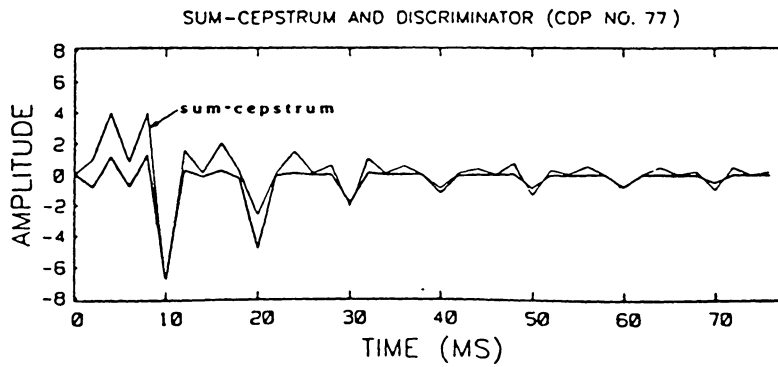
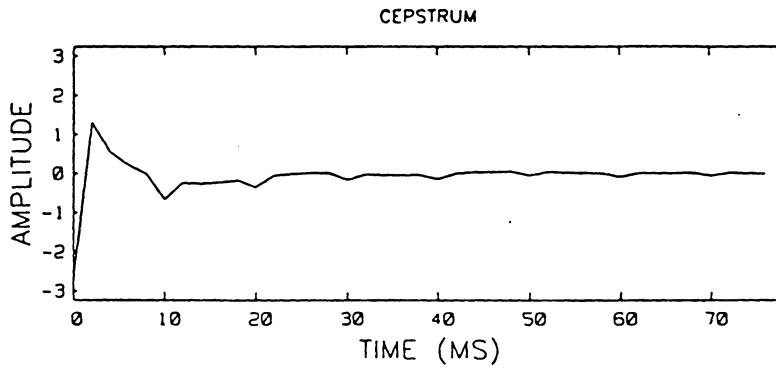
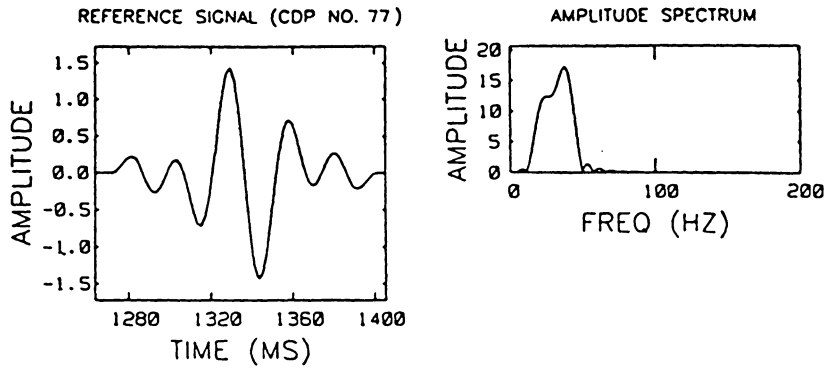


Figure 25. Reflection at CDP 77 ( $dt=2$  ms): The reference signal is the reflection at CDP 77. The sample interval is 2 ms. The sum-cepstrum is based on reflections at CDP's 60 to 75. Increasing the sample rate from 1 ms (Figure 24) to 2 ms has increased the width of the troughs of the sum-cepstrum and the discriminator.

SAMPLE INTERVAL OF 2 MS

TWO-WAY TRAVELTIME OF 10 MS

SUM-CEPSTRUM BASED ON CDP'S 60-75



which synthetic noise was added. If  $s_n(t)$  is a reflection with added noise, then

$$s_n(t) = s(t) + n(t) \quad (28)$$

where  $s(t)$  is the reflection without added noise and  $n(t)$  is the noise.

### Synthetic noise

Synthetic noise was created from random numbers generated by SUBROUTINE URAND (Forsythe et al.(1977, p246)). The amplitude spectrum of each set of random numbers was bandlimited between 5 HZ and 100 HZ. Two examples of sets of random noise are shown in Figure 26. The highest frequency of the bandwidth of the noise lies 1.1 octaves above the highest frequency of the bandwidth of the source wavelet and the lowest frequency of the bandwidth of the noise lies 1.5 octaves below the lowest frequency of the bandwidth of the source wavelet.

### The signal to noise ratio (S/N)

As defined here, the S/N of a synthetic section is the ratio of the maximum root mean squared amplitude of the reflections of the section to the maximum root mean squared amplitude of synthetic noise of the section. For each noise

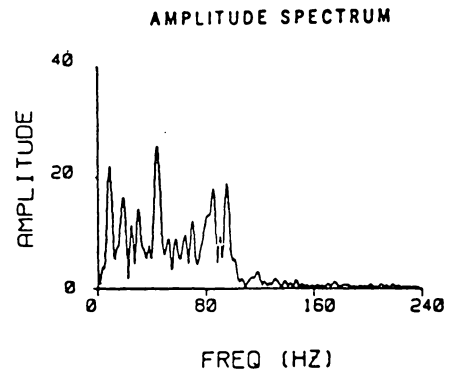
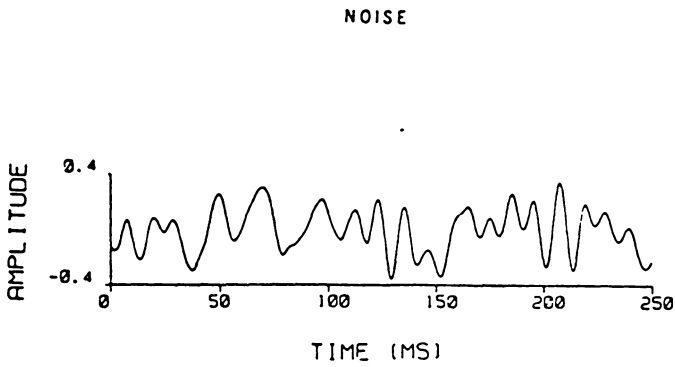
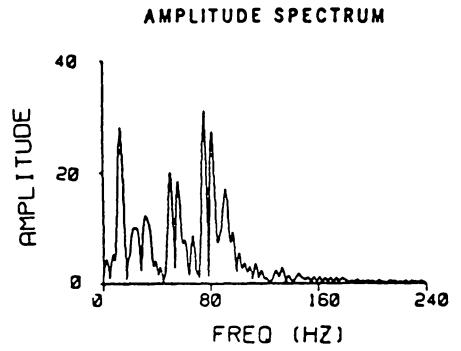
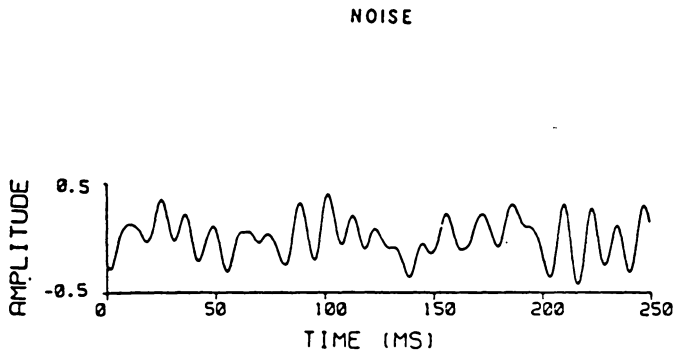


Figure 26. Synthetic noise: Two examples of synthetic noise are shown. The synthetic noise is bandlimited between 5 HZ and 100 HZ.

model, identical series of random numbers were bandlimited and scaled to produce the synthetic noise.

The S/N ratio of the synthetic section is the best S/N ratio of any reflection on the section. Reflections from the middle of the lens have the best S/N ratio, because the root mean squared amplitudes of the reflections are largest. At the edges of the lens, near to CDP's 55 and 110, the root mean squared amplitudes of the reflections are approximately 1/5 the maximum root mean squared amplitude of the reflections. Therefore, at the edges of the lens the S/N ratio is approximately 1/5 the S/N ratio of the section.

#### The noise analysis

Reflections of a synthetic section with a S/N ratio of 15/1 are shown in Figure 27. Because the S/N varies across the section, six different reflections were analyzed. The six reflections are from CDP's 55, 57, 70, 71, 76, and 77. Adjacent or near CDP's were tested to increase the possibility of resolving the two-way traveltime of the lens at each locale. The two-way traveltimes of the lens at the CDP's are; 2 ms at CDP's 55 and 57, 6.5 ms at CDP 70 and 71, and 10 ms at CDP's 76 and 77, thereby representing different thicknesses of the lens.

Reflections at 75 CDP's were used to compute the sum-cepstrum of the six reference signals. The 75 CDP's used are CDP's 2 to 12, 55 to 110, and 121 to 133. These CDP's

NOISE MODEL S/N=15/1

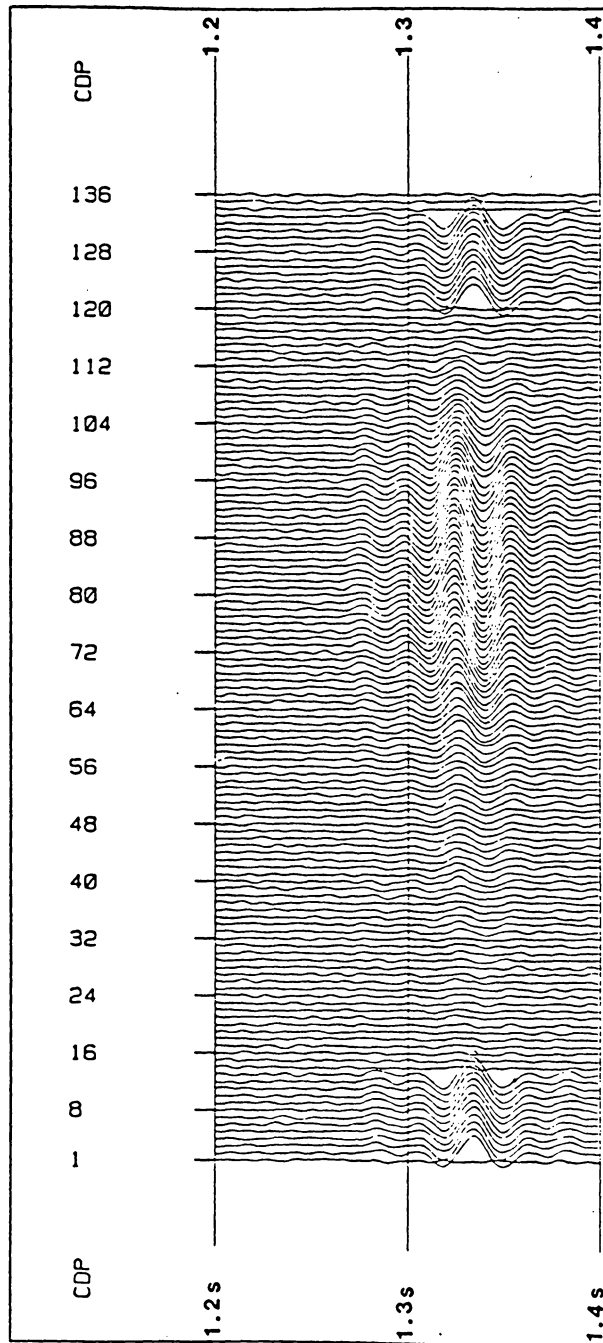


Figure 27. Synthetic section with S/N of 15/1: The sample interval is 1/2 ms.

were chosen because the associated reflections showed the least apparent distortion.

Reflections from model 6 at CDP's 55, 57, 70, 71, 76 and 77 were used as controls for the noise experiments. As with the noisy reflections, the sum-cepstra of the reflections were computed by using the reflections at CDP's 2 to 12, 55 to 110 and 121 to 133. Therefore, any differences between the results obtained from analyses of the noisy reflections and the noise-free reflections is attributed to the synthetic noise.

#### Results of the noise analysis

The accurate two-way traveltime of the lens at each of the six CDP's was recovered from the noise-free reflections by identifying the periods of the troughs of the discriminators. These results are displayed in Figure 28 through Figure 33. The discriminators are typically smooth except for periodic troughs. In these cases the periodicity of the discriminators are obvious and the two-way traveltimes easily determined.

Figure 34 through Figure 39 show the results of the analyses of the reflections with added noise. The first troughs (after 0 ms) of the discriminator are the most reliable for resolving the two-way traveltimes, because as can be seen in the noise-free examples, these troughs have the largest absolute magnitudes. Periodicities were not evident

Figure 28. Reflection without noise; CDP 55: The reflection at CDP 55 of model 6 is the reference signal. The sum-cepstrum is based on reflections at CDP's 2-12, 55-110, and 121-133. Troughs of the discriminator and sum-cepstrum occur at intervals of 2 ms, which is equal to the two-way traveltime of the lens at CDP 55.

SAMPLE INTERVAL OF 1/2 MS

TWO-WAY TRAVELTIME OF 2 MS

SUM-CEPSTRUM BASED ON CDP'S 2-12.  
55-110 & 121-133

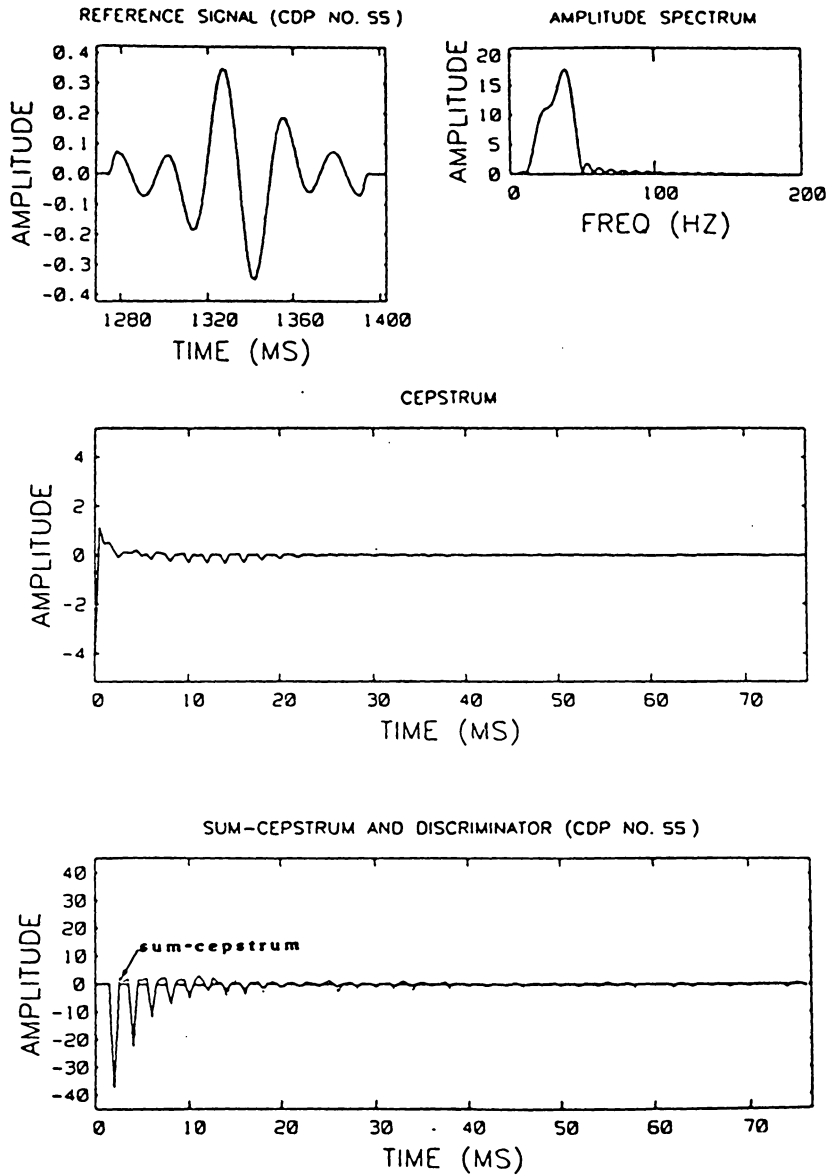


Figure 29. Reflection without noise; CDP 57: The reflection at CDP 57 of model 6 is the reference signal. The sum-cepstrum is based on reflections at CDP's 2-12, 55-110, and 121-133. Troughs of the discriminator and the sum-cepstrum occur at intervals of 2 ms, which is equal to the two-way traveltime of the lens at CDP 57.

SAMPLE INTERVAL OF 1/2 MS

TWO-WAY TRAVELTIME OF 2 MS

SUM-CEPSTRUM BASED ON CDP'S 2-12,  
55-110 & 121-133

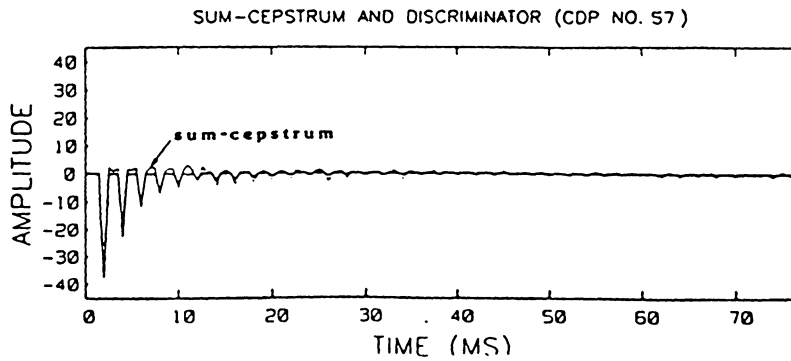
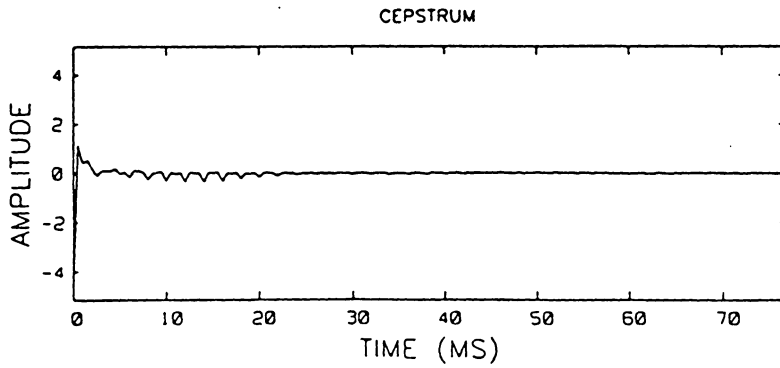
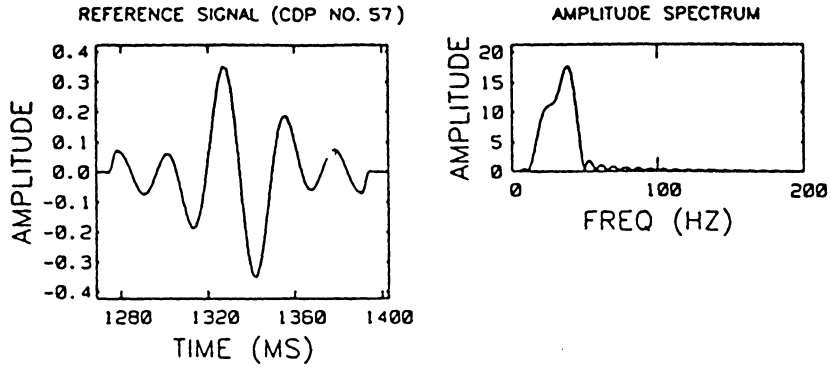


Figure 30. Reflection without noise; CDP 70: The reflection at CDP 70 of model 6 is the reference signal. The sum-cepstrum is based on reflections at CDP's 2-12, 55-110, and 121-133. Troughs of the discriminator and the sum-cepstrum occur at intervals of 6.5 ms, which is equal to the two-way traveltime of the lens at CDP 70.

SAMPLE INTERVAL OF 1/2 MS

TWO-WAY TRAVELTIME OF 6.5 MS

SUM-CEPSTRUM BASED ON CDP'S 2-12,  
55-110 & 121-133

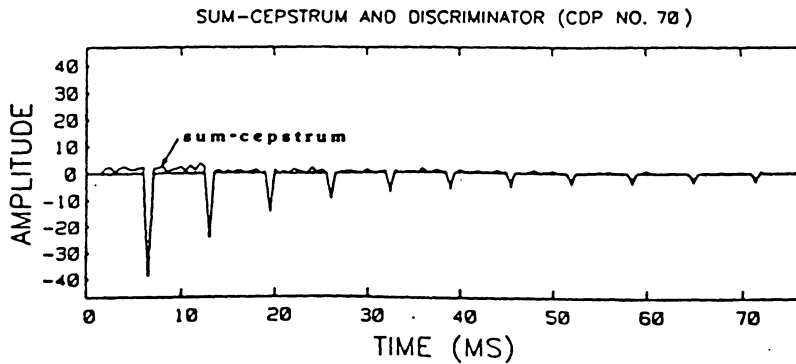
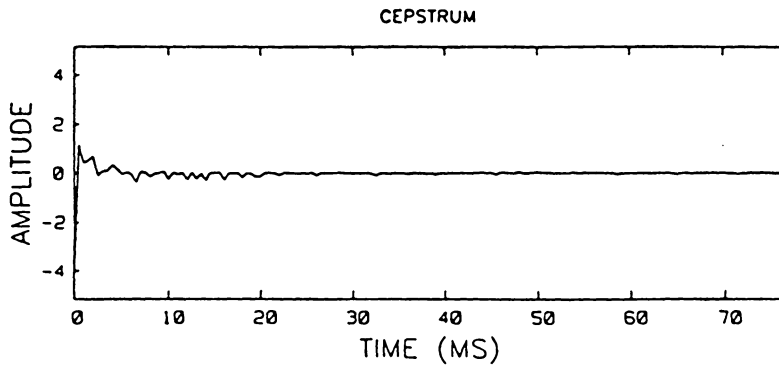
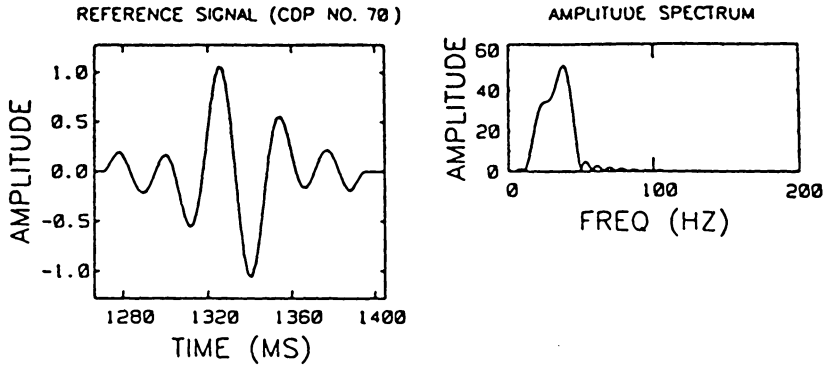


Figure 31. Reflection without noise; CDP 71: The reflection at CDP 71 of model 6 is the reference signal. Troughs of the discriminator and the sum-cepstrum occur at intervals of 6.5 ms, which is equal to the two-way traveltime of the lens at CDP 70.

SAMPLE INTERVAL OF 1/2 MS

TWO-WAY TRAVELTIME OF 6.5 MS

SUM-CEPSTRUM BASED ON CDP'S 2-12,  
55-110 & 121-133

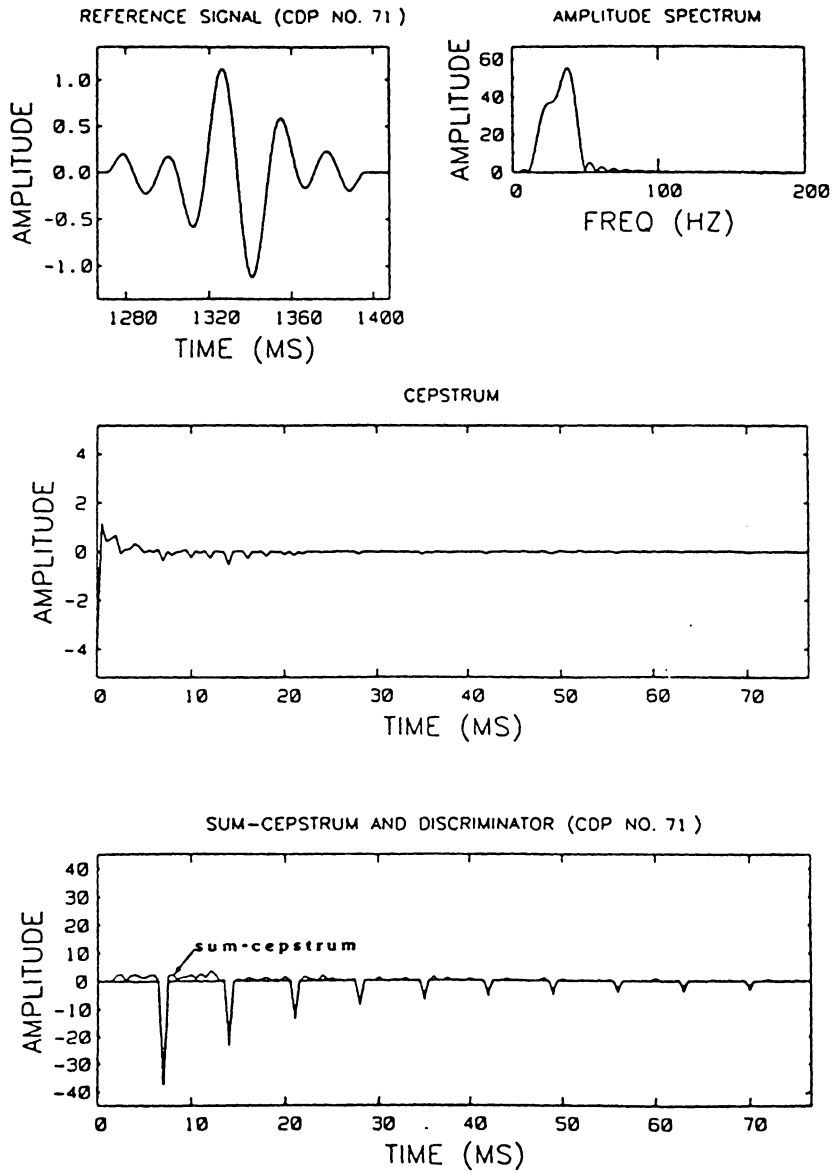


Figure 32. Reflection without noise; CDP 76: The reflection at CDP 76 of model 6 is the reference signal. The sum-cepstrum is based on reflections at CDP's 2-12, 55-110, and 121-133. Troughs of the discriminator and the sum-cepstrum occur at intervals of 10 ms, which is equal to the two-way traveltime of the lens at CDP 70.

SAMPLE INTERVAL OF 1/2 MS

TWO-WAY TRAVELTIME OF 10 MS

SUM-CEPSTRUM BASED ON CDP'S 2-12,  
55-110 & 121-133

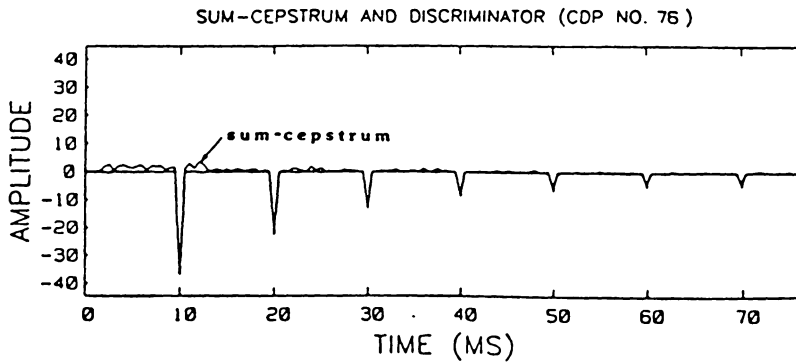
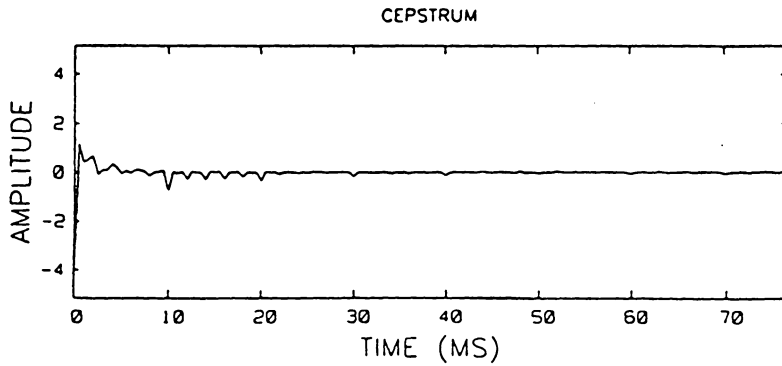
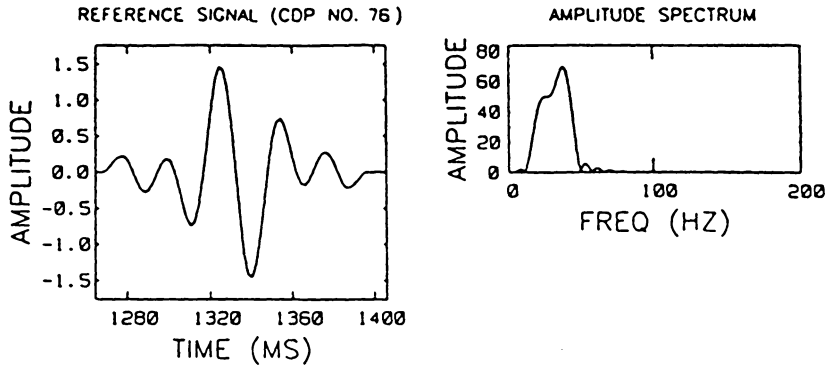
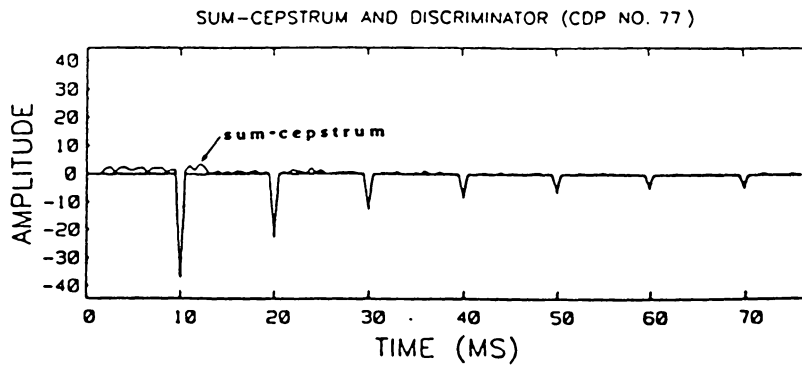
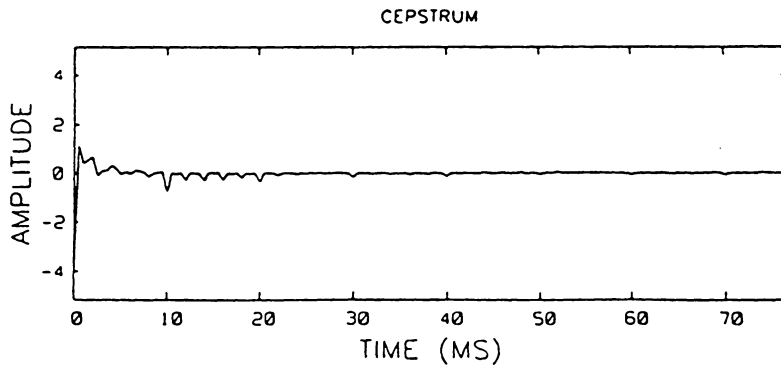
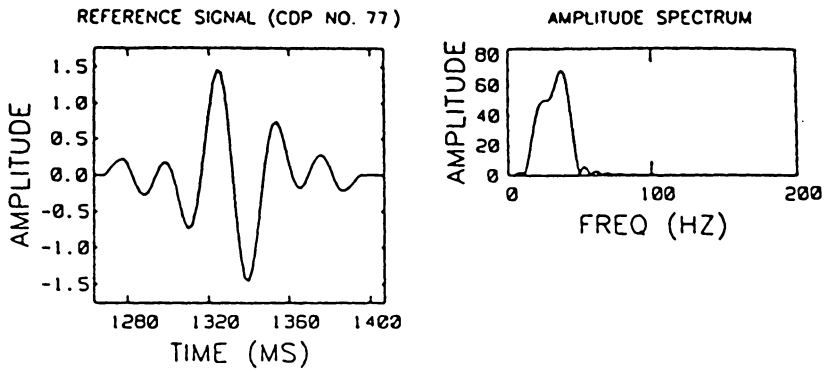


Figure 33. Reflection without noise; CDP 77: The reflection at CDP 77 of model 6 is the reference signal. The sum-cepstrum is based on reflections at CDP's 2-12, 55-110, and 121-133. Troughs of the discriminator and the sum-cepstrum occur at intervals of 10 ms, which is equal to the two-way traveltime of the lens at CDP 77.

SAMPLE INTERVAL OF 1/2 MS

TWO-WAY TRAVELTIME OF 10 MS

SUM-CEPSTRUM BASED ON CDP'S 2-12,  
55-110 & 121-133



in the discriminators of the reflections at CDP's 71 (Figure 37), and 77 (Figure 39); therefore the two-way traveltimes could not be determined. In the discriminators of the reflections at CDP's 55 (Figure 34) and 57 (Figure 35), the first three troughs occur at 1.6 ms, 4.0 ms and 6.0 ms, and 1.5 ms, 4.0 ms, and 6.0 ms, respectively. In each case the troughs lie within 1 sample interval of integer multiples of the two-way traveltime of 2 ms. Therefore the two-way traveltime at CDP's 55 and 57 are resolved as periods of 2 ms within the corresponding discriminators. In addition, the discriminator of the reference signal at CDP 70 (Figure 36) has troughs at 6.5 ms and 13 ms, which indicates a two-way traveltime of 6.5 ms. Similarly the discriminator of the reference signal at CDP 76 (Figure 38) has troughs at 10 ms and 20 ms, which indicates a two-way traveltime of 10 ms.

Although the two-way traveltimes were resolved for the reference signals at CDP's 55, 57, 70 and 77, noise has severely reduced the resolution in the quefreny domain. The analyses show that because of added noise, the cepstrum of the source wavelet was not completely removed.

Jin and Rogers (1983) showed how the effects of noise on homomorphic deconvolution can be expressed analytically. A similar approach is taken here to explain the degradation of the sum-cepstrum by the synthetic noise. From equation (28), the Fourier transform of  $s_n(t)$  is;

Figure 34. Reflection with added noise; CDP 55: The reflection at CDP 55 of the noise section is the reference signal. The sum-cepstrum is based on reflections at CDP's 2-12, 55-110, and 121-133. In the discriminator troughs occur at 1.6 ms, 4.0 ms and 6.0 ms (see short arrows). Each trough lies within one sample interval of integer multiples of the two-way traveltime of 2 ms, therefore the two-way traveltime of 2 ms has been resolved. Note that the discriminator and sum-cepstrum are shown between times 0.5 ms and 77 ms. The inset shows the functions between 0 ms to 76 ms. The same arrangements are maintained in Figure 35 to Figure 39.

REFLECTION WITH ADDED NOISE

SAMPLE INTERVAL OF 1/2 MS

TWO-WAY TRAVELTIME OF 2 MS

SUM-CEPSTRUM BASED ON CDP'S 2-12,  
55-110 & 121-133

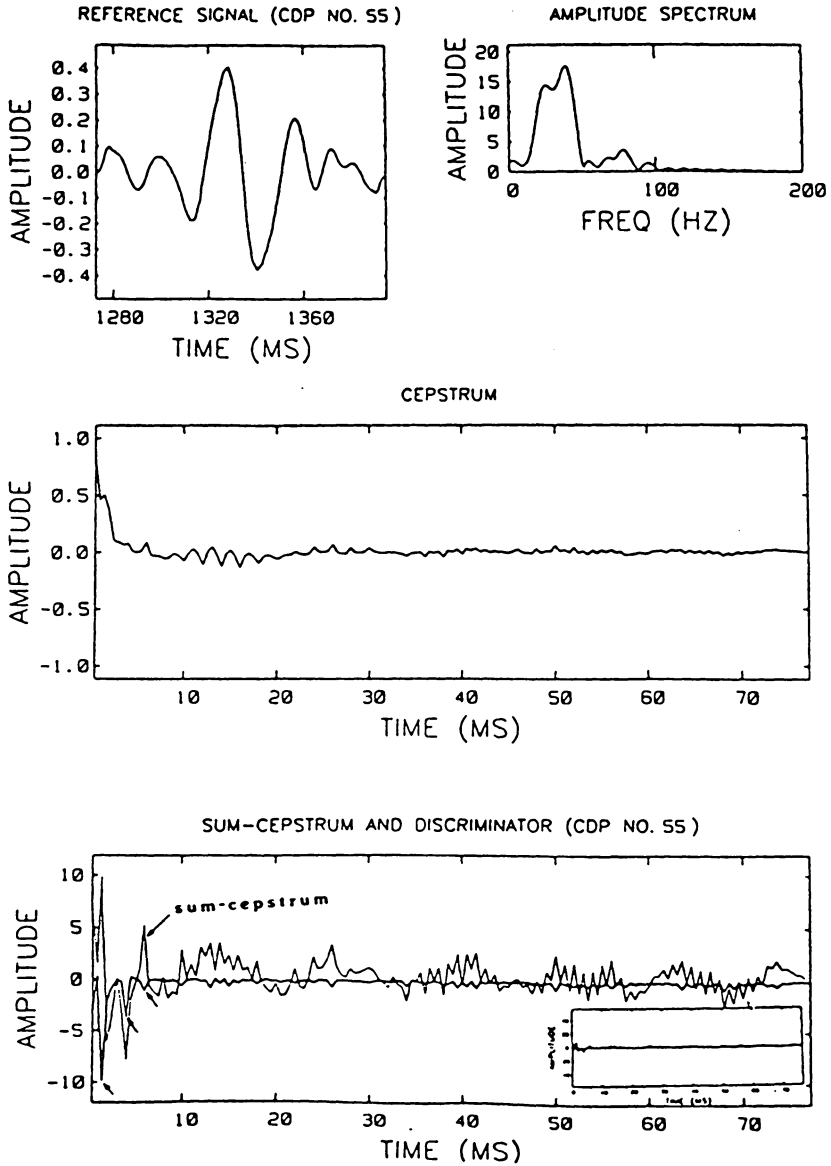


Figure 35. Reflection with added noise; CDP 57: The reflection at CDP 57 of the noise section is the reference signal. The sum-cepstrum is based on reflections at CDP's 2-12, 55-110, and 121-133. In the discriminator troughs occur at 1.5 ms, 4.0 ms and 6.0 ms. (see short arrows). Each trough lies within one sample interval of integer multiples of the two-way traveltime of 2 ms, therefore the two-way traveltime has been resolved.

REFLECTION WITH ADDED NOISE

SAMPLE INTERVAL OF 1/2 MS

TWO-WAY TRAVELTIME OF 2 MS

SUM-CEPSTRUM BASED ON CDP'S 2-12,  
55-110 & 121-133

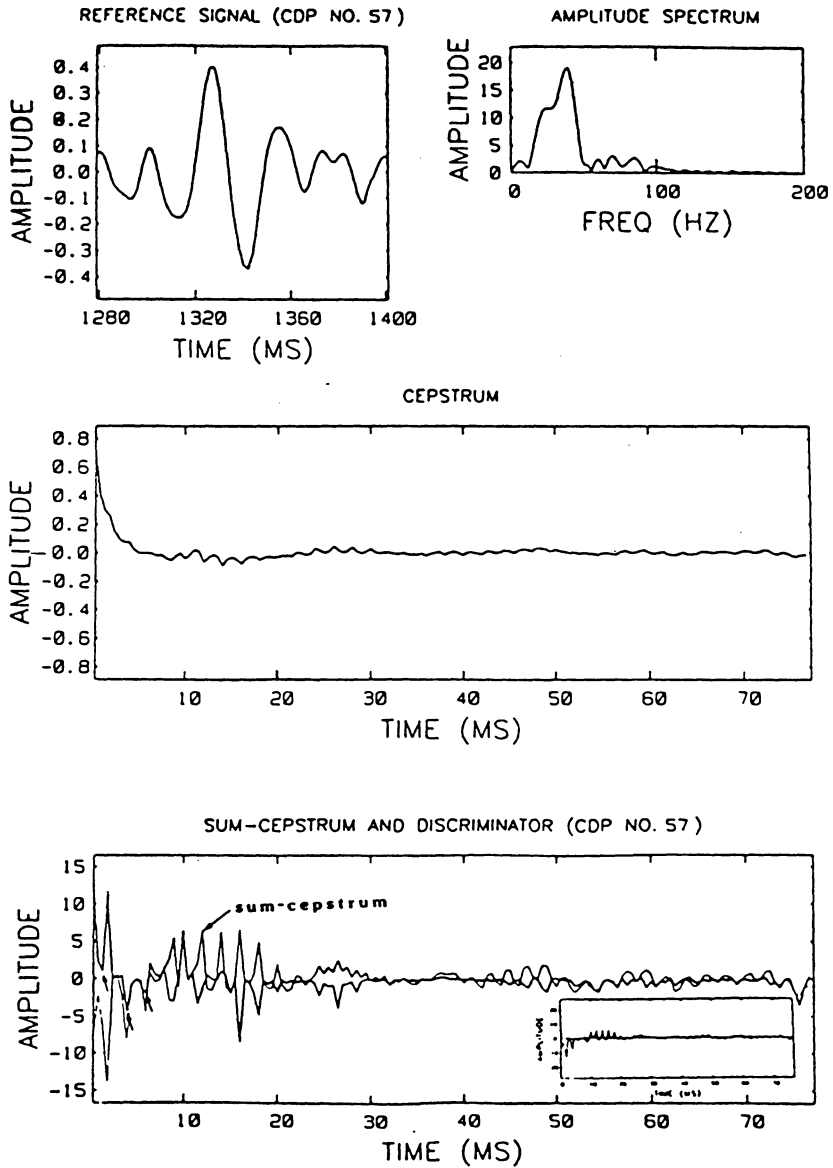


Figure 36. Reflection with added noise; CDP 70: The reflection at CDP 70 of the noise section is the reference signal. The sum-cepstrum is based on reflections at CDP's 2-12, 55-110, and 121-133. In the discriminator troughs occur at 6.5 ms and 13 ms (see short arrows), therefore the two-way traveltime of 6.5 ms has been resolved.

REFLECTION WITH ADDED NOISE

SAMPLE INTERVAL OF 1/2 MS

TWO-WAY TRAVELTIME OF 6.5 MS

SUM-CEPSTRUM BASED ON CDP'S 2-12,  
55-110 & 121-133

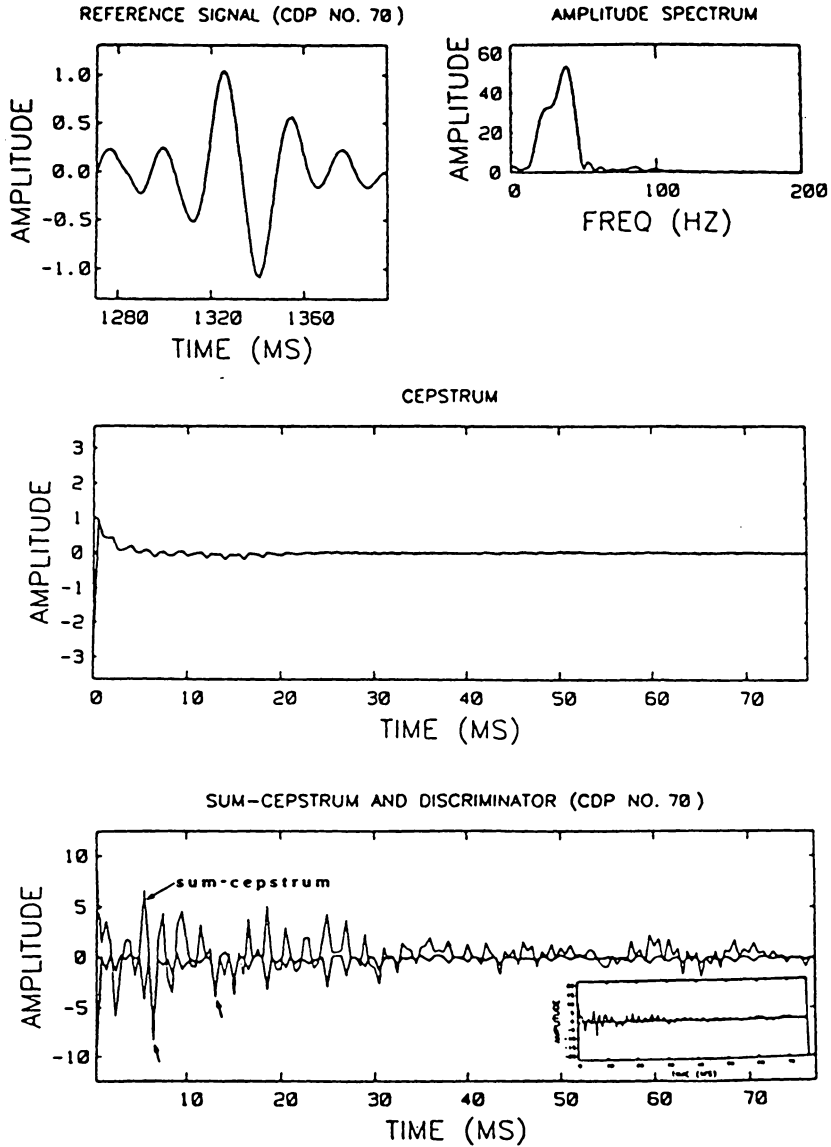


Figure 37. Reflection with added noise; CDP 71: The reflection at CDP 71 of the noise section is the reference signal. The sum-cepstrum is based on reflections at CDP's 2-12, 55-110, and 121-133. The discriminator does not indicate a periodicity within the sum-cepstrum, therefore the two-way traveltime of 10 ms has not been resolved.

REFLECTION WITH ADDED NOISE

SAMPLE INTERVAL OF 1/2 MS

TWO-WAY TRAVELTIME OF 6.5 MS

SUM-CEPSTRUM BASED ON CDP'S 2-12,  
55-110 & 121-133

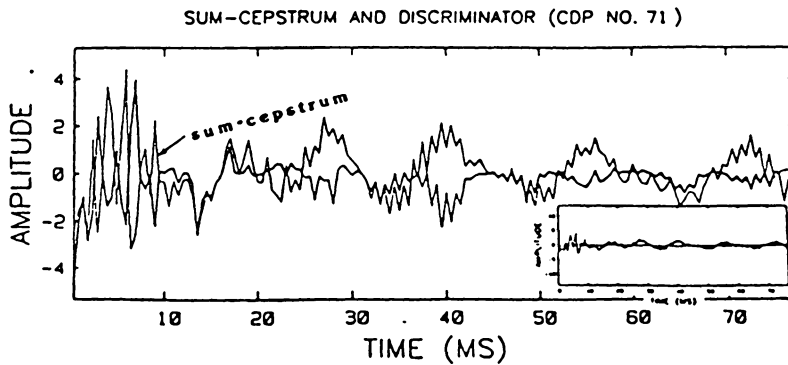
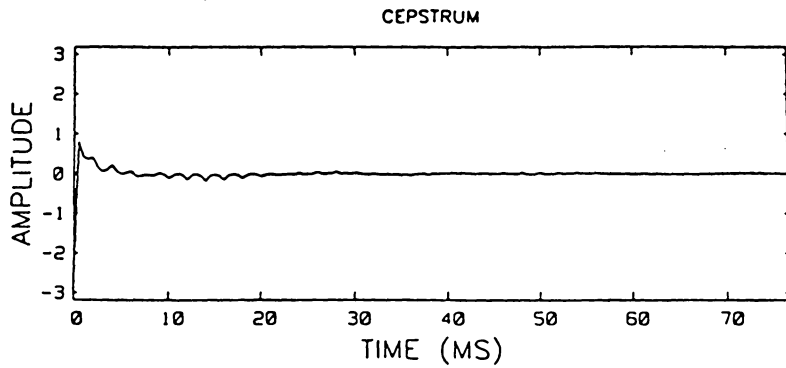
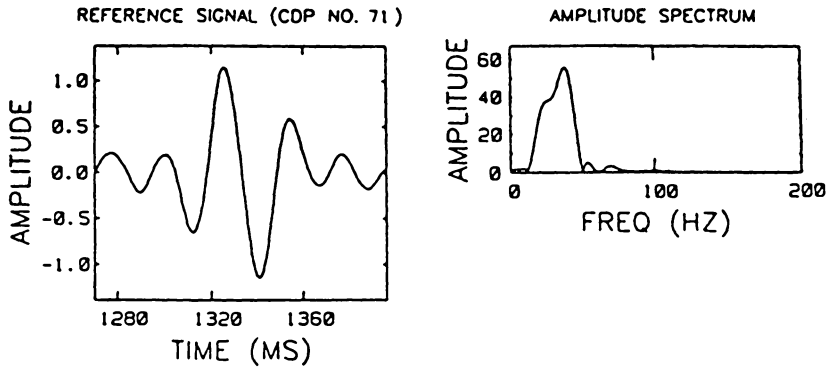


Figure 38. Reflection with added noise; CDP 76: The reflection at CDP 76 of the noise section is the reference signal. The sum-cepstrum is based on reflections at CDP's 2-12, 55-110, and 121-133. In the discriminator troughs occur at 10 ms and 20 ms (see short arrows), therefore the two-way traveltime of 10 ms has been resolved.

REFLECTION WITH ADDED NOISE

SAMPLE INTERVAL OF 1/2 MS

TWO-WAY TRAVELTIME OF 10 MS

SUM-CEPSTRUM BASED ON CDP'S 2-12,  
55-110 & 121-133

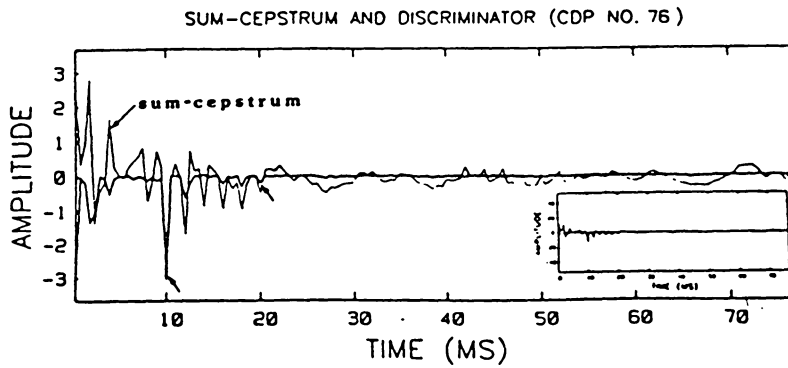
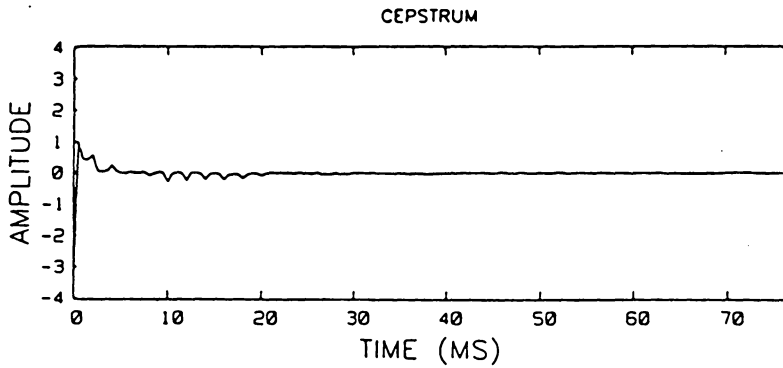
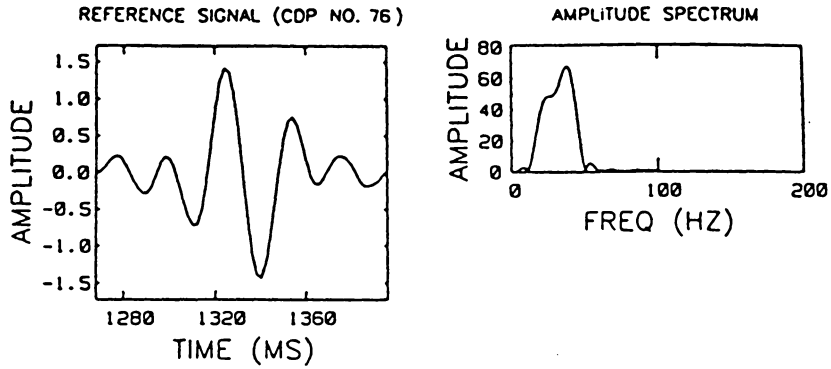


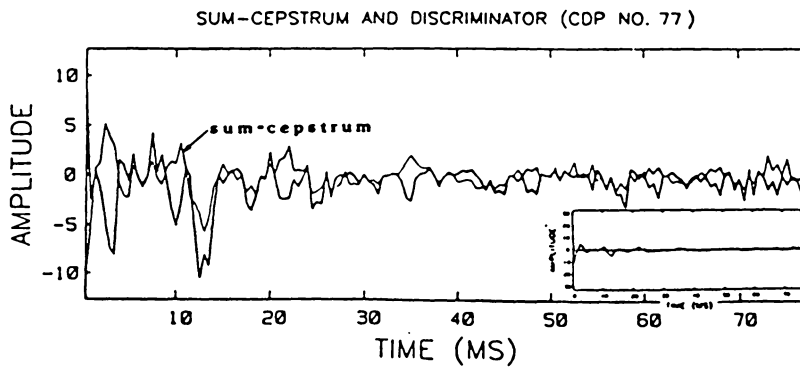
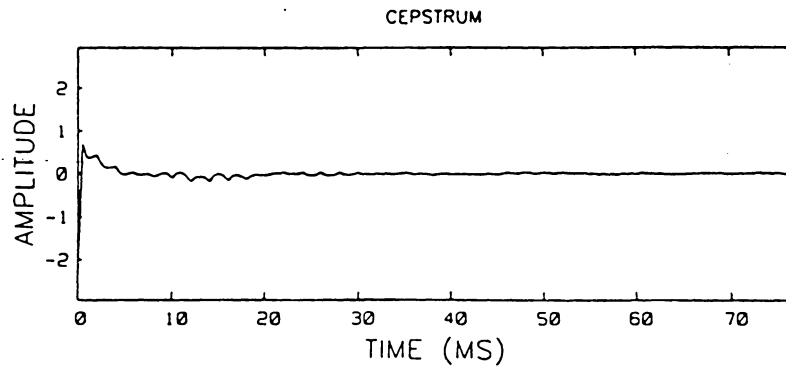
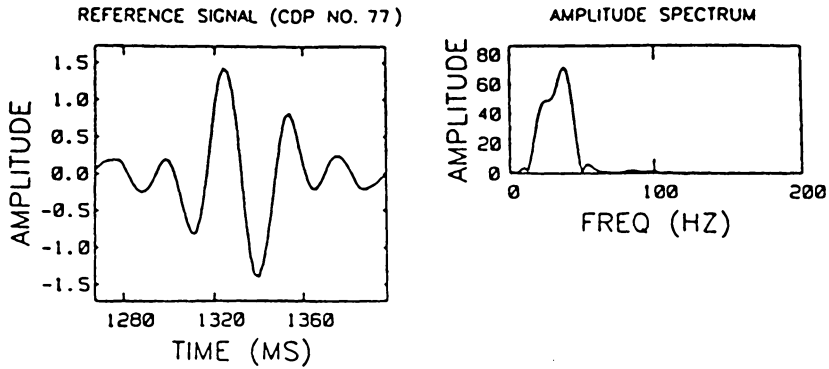
Figure 39. Reflection with added noise; CDP 77: The reflection at CDP 77 of the noise section is the reference signal. The sum-cepstrum is based on reflections at CDP's 2-12, 55-110, and 121-133. The discriminator does not indicate a periodicity within the sum-cepstrum; therefore the two-way traveltime of 10 ms is not resolved.

REFLECTION WITH ADDED NOISE

SAMPLE INTERVAL OF 1/2 MS

TWO-WAY TRAVELTIME OF 10 MS

SUM-CEPSTRUM BASED ON CDP'S 2-12,  
55-110 & 121-133



$$S_n(\omega) = S(\omega) + N(\omega) \quad (29)$$

where  $S_n(\omega)$  is the Fourier transform of  $s_n(t)$ , and  $N(\omega)$  is the Fourier transform of  $n(t)$ . The Fourier transform of the cepstrum of the reflection is

$$C_n(\omega) = \ln(|S(\omega) + N(\omega)|) \quad (30)$$

If

$$|N(\omega)| \ll |S(\omega)| \quad (31)$$

for all frequencies of  $s_n(t)$ , then

$$C_n(\omega) \approx C(\omega) \quad (32)$$

where  $C(\omega)$  is the Fourier transform of the cepstrum of  $s(t)$ . Therefore if equations (31) and (32) are true then

$$c_n(t) \approx c(t) \quad (33)$$

However if

$$|N(\omega)| \approx |S(\omega)| \quad (34)$$

or

$$|N(\omega)| \gg |S(\omega)| \quad (35)$$

for some or all frequencies of  $s(t)$ , equation (32) is not true. In this case it is not expected that the cepstrum of the source wavelet will be completely removed when the sub-cepstrum is computed. Equation (34) and (35) hold for some of the reflections used in the noise analysis; for example, those at CDP's 71 (Figure 37), and 77 (Figure 39). Specifically, frequencies outside the bandwidth of the main lobe of the amplitude spectrum of the reflections were severely altered by noise. However as with the reflections at CDP's 55 (Figure 34), 57 (Figure 35), 70 (Figure 36) and 76 (Figure 38),  $|S(\omega)|/|N(\omega)|$  was large enough at each frequency,  $\omega$ , to enable the detection of the two-way traveltime of the lens at these CDP's.

## SUMMARY AND CONCLUSION

A method of cepstrum analysis was developed for the purpose of resolving the thickness of thin-beds. The method relies on the detection of periodic pulses in the cepstra of reflectivity functions, which are isolated by computing the sub-cepstrum and sum-cepstrum and highlighted with the discriminator. Studies were performed by applying the method to synthetic thin lens models.

The method is sensitive to the ratio of reflection coefficients of the reflectivity function. Specifically, it was determined that the resolution depends on the ratio of the reflection coefficients; for example, optimum resolution is achieved when  $|R_0| = |R_1|$ . In addition, in the noise-free case, the magnitude of the cepstral pulses can be used to determine the magnitude of the ratio of the reflection coefficients. For example by equations (15) and (16), when  $|R_0| = |R_1|$  the cepstrum of the reflectivity function will have non-zero values of 0.5, 0.25, 0.125, ...etc. Although the technique is sensitive to the magnitude of the ratio of the reflection coefficients it cannot distinguish between a high speed layer and a low speed layer.

The technique is also sensitive to the sample interval. The finest sample interval provides the best resolution be-

•  
cause it produces the the sharpest cepstral pulses and is able to resolve the thinnest beds.

During the noise analysis it was shown that the method is adversely affected by noise when  $|N(\omega)| \gg |S(\omega)|$  for some frequencies of the signal. Whatever the S/N, this condition will more likely happen outside the spectral bandwidth of the signal. Therefore it is hypothesized that the method will be more successful with a broadband wavelet.

Of the six reflections examined during the noise analysis, the correct two-way traveltimes were recovered from the four at CDP's 55, 57, 70 and 76. However, the two-way traveltime obtained from these reflections provided useful information about the geology. For example, the two-way traveltimes indicated that there was a thin-bed present which was thinning towards the left edge of model 6, from a two-way traveltime thickness of 10 ms at CDP 76 to a two-way traveltime thickness of 2 ms at CDP 55. In brief; because the method would be applied with multi-trace data, success need be achieved with only some of those traces to provide vital information about the geology.

## PROPOSAL FOR FUTURE STUDIES

The method of analysis, like most other methods, was adversely affected by noise. For a further study, elimination of the effect of noise on the discriminator is suggested. It seems that the noise problem could be addressed by stacking near reflections from a suspected thin-bed where the thin-bed does not rapidly nor continuously change thickness (wave shapes not quickly changing). The method would then be applied to the stacked reflections which would have an improved S/N ratio. Indeed, the application of stacking to improve the effectiveness of homomorphic deconvolution has been applied successfully in earthquake studies by Kemerait and Sutton (1982). Similarly, Otis and Smith (1977) also found that a form of stacking, which they called log spectral averaging, enhanced the results of homomorphic deconvolution. Because of the basic similarity between homomorphic deconvolution and cepstrum analysis (they are both based on the theory of homomorphic systems), it is expected that correct application of stacking can improve the effectiveness of cepstrum analysis.

Of course there are other potential problems besides random noise to be considered. Eventually the effects of the following systems must be studied; the earth filter as a

time-variant attenuator, instrument responses, interbed multiples ... and more.

Finally the method must be tested with real data. The seismic data considered most suitable for the method of analysis is high-fold marine data for which the S/N ratio is high and in which reflections from isolated horizontal thinbeds are contained.

## REFERENCES

- B. P. Bogert, M. J. R. Healy, and J. W. Tukey, "The Quefrequency Alanysis of Time Series for Echoes: Cepstrum, Pseudo-autocovariance, Cross-Cepstrum and Saphe Crack-ing", Proceedings of the Symposium on Time Series Analy-sis, M. Rosenblatt, Ed., John Wiley and Sons, Inc., New York, 1963, pp209-243.
- P. Buhl, P. L. Stoffa, and G. Bryan, "The Application of Homomorphic Deconvolutin To Shallow-Water Marine Seismology--Part 2: Real Data", Geophysics, vol. 39, no. 4, 1974, p. 417-426.
- D. G. Childers, D. P. Skinner, and R. C. Kemerait, "The Cepstrum: A guide to Processing", Proceedings of the IEEE, vol. 65, no. 10, October 1977, p. i428-1443.
- G. Forsythe, M. Malcolm, and C. Moler, Computer Methods For Mathematical Computations, Prentice Hall, Inc., New Jersey, 1977, 259 pp.
- GeoQuest International, Inc., Advance Interpretative Model-ing System AIMS® Users Reference Manual, GeoQuest Inter-national Inc., Houston, Texas, 1983.
- D. J. Jin and E. Eisner, "A Review of Homomorphic Deconvo-lution", Reviews of Geophysics and Space Physics, vol. 22, no. 3, August 1984, pp. 255-263.
- D. J. Jin and J. R. Rogers, "Homomorphic Deconvolution", Geophysics, vol. 48, no. 7, July 1983, p.1014-1016.
- R. C. Kemerait and A. F. Sutton, "A Multidimensional Approach to Seismic Event Depth Estimation", Geoexploration, vol. 20, 1982, p. 113-130
- R. M. Otis and R. B. Smith, "Homomorphic Deconvolution By Log Spectral Averaging", Geophysics, vol. 42, no. 6, October 1977, pp. 1146-1157.
- M. Lane, and T. Ulrych, "Discussion" [on 'Homomorphic Decon-volution' by D. J. Jin and J. R. Rogers], Geophysics, vol. 49, no. 9, September 1984, pp. 1559-1560, with Reply to "Discussion" by D. J. Jin pp. 1561.
- Alan Oppenheim and Ronald Schafer, Digital Signal Processing, Prentice-Hall Inc., New Jersey, 1975, 585 pp.

P. L. Stoffa, P. Buhl, and G. Bryan, "The Application of Homomorphic Deconvolution To Shallow-Water Marine Seismology--Part 1: Models", *Geophysics*, vol. 39, no. 4, 1974, pp. 401-416.

Jose Manuel Tribolet, Applications of Homomorphic Signal Processing, Prentice-Hall Inc., New Jersey, 1979, 195 pp.

T. J. Ulrych, "Application of Homomorphic Deconvolution to Seismology", *Geophysics*, vol. 36, no. 4, August 1971, pp. 650-660.

T. J. Ulrych, O. G. Jensen, R. M. Ellis, and P. G. Somerville, "Homomorphic Deconvolution of Some Teleseismic Events", *Bulletin of the Seismological Society of America*, vol. 62, no. 5, October 1972, pp. 1269-1281

M. B. Widess, "How Thin is a Thin Bed", *Geophysics*, vol. 38, no. 6, December 1973, pp. 1176-1180.

**The vita has been removed from  
the scanned document**